2-2011

Structural Evolution of a Composite Middle to Lower Crustal Section: The Sierra de Pie de Palo, Northwest Argentina

Sean R. Mulcahy
Western Washington University, sean.mulcahy@wwu.edu

S. M. Roeske

W. C. McClelland

F. Jourdan

A. Iriondo

See next page for additional authors

Structural evolution of a composite middle to lower crustal section: The Sierra de Pie de Palo, northwest Argentina

S. R. Mulcahy,[1,2] S. M. Roeske,[3] W. C. McClelland,[4] F. Jourdan,[5,6] A. Iriondo,[7] P. R. Renne,[6,8] J. D. Vervoort,[9] and G. I. Vujovich[10]

Received 22 December 2009; revised 14 October 2010; accepted 27 October 2010; published 27 January 2011.

[1] The Sierra de Pie de Palo of northwest Argentina preserves middle to lower crustal metamorphic rocks that were penetratively deformed during Ordovician accretion of the Precordillera terrane to the Gondwana margin. New structural, petrologic, and geochronologic data from a 40 km structural transect reveals that the Sierra de Pie de Palo preserves a middle to lower crustal ductile thrust complex consisting of individual structural units and not an intact ophiolite and cover sequence. Top-to-the-west thrusting occurred intermittently on discrete ductile shear zones from ~515 to ~417 Ma and generally propagated toward the foreland with progressive deformation. Ordovician crustal shortening and peak metamorphic temperatures in the central portion of the Sierra de Pie de Palo were synchronous with retro-arc shortening and magmatic flare-up within the Famatina arc. Accretion of the Precordillera terrane resulted in the end of arc flare-up and the onset of synconvergent extension by ~439 Ma. Continued synextensional to postextensional convergence was accommodated along progressively lower grade shear zones following terrane accretion and the establishment of a new plate margin west of the Precordillera terrane. The results support models of Cordilleran orogens that link voluminous arc magmatism to periods of regional shortening. The deformation, metamorphic, and magmatic history within the Sierra de Pie de Palo is consistent with models placing the region adjacent to the Famatina margin in the middle Cambrian and not as basement to the Precordillera terrane. **Citation:** Mulcahy, S. R., S. M. Roeske, W. C. McClelland, F. Jourdan, A. Iriondo, P. R. Renne, J. D. Vervoort, and G. I. Vujovich (2011), Structural evolution of a composite middle to lower crustal section: The Sierra de Pie de Palo, northwest Argentina, *Tectonics*, *30*, TC1005, doi:10.1029/2009TC002656.

1. Introduction

[2] Continental crust is created, deformed, and destroyed at convergent margins. Within Cordilleran-like orogenic systems, short-lived (~10–20 Myr) voluminous arc magmatism, regional crustal shortening, and arc-root foundering are hypothesized to be linked processes [e.g., *Ducea*, 2001; *Ducea and Barton*, 2007]. In such a model, arc flare-up, fore-arc and retro-arc shortening, and delamination may repeat cyclically unless interrupted by processes such as shifts in plate motion, changes in the amount or type of underthrust material, or by terrane accretion [*DeCelles et al.*, 2009]. Testing models of such linked processes requires detailed structural mapping, petrology, and geochronology from active and ancient convergent margins.

[3] The western Sierras Pampeanas of northwest Argentina (Figure 1) preserve the evolution from a Cambrian convergent margin to an Ordovician collisional orogen [*Astini et al.*, 1995; *Mulcahy et al.*, 2007]. The Cambrian Famatina arc initiated as an Andean style continental arc through east dipping subduction of Iapetan oceanic lithosphere as early as ~515–495 Ma [*Pankhurst and Rapela*, 1998; *Pankhurst et al.*, 2000; *Quenardelle and Ramos*, 1999; *Mulcahy et al.*, 2007]. The majority of the magmatic activity occurred over a short time interval from ~485 to 465 Ma [*Ducea et al.*, 2010]. Within the allochthonous Precordillera terrane, stratigraphic evidence suggests that the terrane fully collided with the Famatina arc margin by ~470–465 Ma [e.g., *Astini et al.*, 1995; *Fanning et al.*, 2004] coincident with the cessation of voluminous arc magmatism. While both the magmatic history of the arc and the subsidence history of the Precordillera terrane are well documented, the deformation history within the Famatina margin is poorly understood.

[4] Located between the Precordillera terrane and the Cambrian-Ordovician Famatina arc (Figure 1), greenschist through granulite facies metamorphic rocks of the Sierra de Pie de Palo have been interpreted to preserve a metamorphosed Mesoproterozoic oceanic basement and younger cover sequence [*Ramos et al.*, 1998; *Vujovich and Kay*, 1998; *Casquet et al.*, 2001] that experienced polyphase metamor-

[1]Department of Geoscience, University of Nevada, Las Vegas, Las Vegas, Nevada, USA.
[2]Now at Department of Earth and Planetary Sciences, University of California, Berkeley, California, USA.
[3]Department of Geology, University of California, Davis, California, USA.
[4]Department of Geoscience, University of Iowa, Iowa City, Iowa, USA.
[5]Western Australian Argon Isotope Facility, Department of Applied Geology and JdL-CMS, Curtin University of Technology, Perth, Western Australia, Australia.
[6]Berkeley Geochronology Center, Berkeley, California, USA.
[7]Centro de Geociencias, Universidad Nacional Autónoma de México, Querétaro, Mexico.
[8]Department of Earth and Planetary Science, University of California, Berkeley, California, USA.
[9]School of Earth and Environmental Sciences, Washington State University, Pullman, Washington, USA.
[10]Department of Geology, University of Buenos Aires-CONICET, Buenos Aires, Argentina.

0278-7407/11/2009TC002656

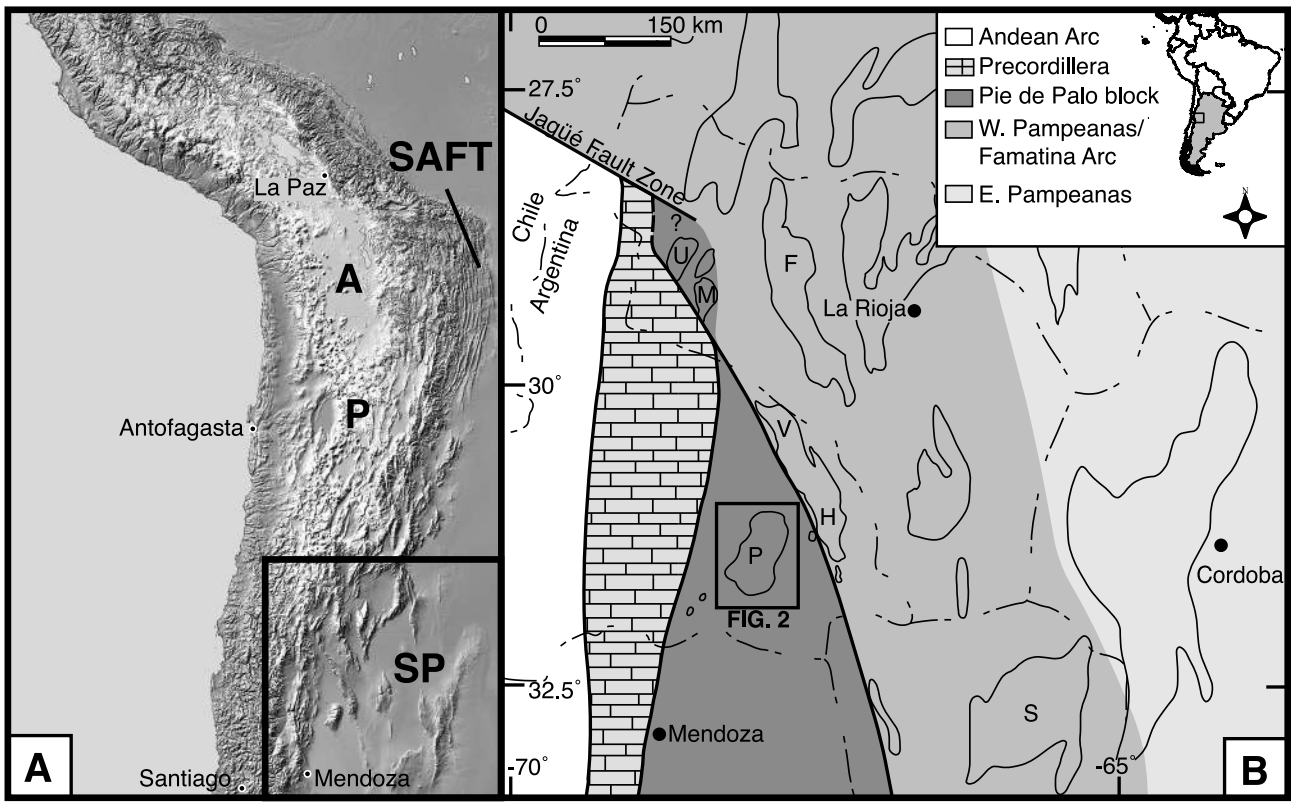

Figure 1. (a) Shaded relief map of western South America illustrating the geographic location of the study area within the Sierras Pampeanas (SP). Geologic provinces labeled for reference are the Altiplano (A) and Puna plateau (P) and the Southern Andean fold and thrust belt (SAFT). (b) Tectonic map of northwest Argentina. Thick lines mark intraterrane boundaries, and thin dash-dotted lines mark country and province boundaries. Individual ranges shown for reference are F, Sierras de Famatina; H, Sierras de la Huerta; M, Sierras de Maz; P, Sierras de Pie de Palo; S, Sierras de San Luis; U, Sierra de Umango; V, Valle Fértil.

phism and deformation [*Dalla Salda and Varela*, 1984; *Ramos et al.*, 1998; *van Staal et al.*, 2010]. Two competing hypotheses exist for the affinity of the Sierra de Pie de Palo. The most commonly held view considers the entire Sierra de Pie de Palo as the basement to Precordillera terrane and to have undergone penetrative Ordovician deformation during the accretion of the Precordillera to the Famatina arc margin [*Ramos*, 2004, and references therein; *van Staal et al.*, 2010]. An alternative view considers rocks of the Sierra de Pie de Palo (with the exception of the Caucete Group, described below) as separate from the Precordillera terrane and to have been adjacent with the Famatina margin by ~515 Ma [*Mulcahy et al.*, 2007]. The latter interpretation is based on a Cambrian mylonite event preserved within the Sierra de Pie de Palo and magmatic and metamorphic ages within the Famatina arc–fore-arc margin [*Mulcahy et al.*, 2007]. The two scenarios predict distinctly different deformation and thermal histories within the Sierra de Pie de Palo.

[5] We combine structural mapping, thermobarometery, and geochronology using multiple isotopic systems to constrain the petrologic and tectonic settings of major structures within the Sierra de Pie de Palo and to constrain the relative and absolute timing of deformation on those structures. The data support exiting models of Cordilleran margins that invoke arc flare-up linked to episodes of regional shortening. The magmatic and deformation history within the Sierra de Pie de Palo is consistent with models placing the Sierra de Pie de Palo adjacent to the Famatina margin by the middle to late Cambrian and not as the basement to the Precordillera terrane.

2. Geology of the Sierra de Pie de Palo

[6] We recognize four structurally bounded units within the Sierra de Pie de Palo that are separated based largely on lithology and metamorphic grade (Figure 2). From the west to the east, they are the Caucete Group, the Pie de Palo Complex, the Central Complex, and the Nikizanga Group.

[7] The Caucete Group [e.g., *Ramos et al.*, 1996, 1998; *Vujovich and Kay*, 1998; *Casquet et al.*, 2001; *Galindo et al.*, 2004; *van Staal et al.*, 2010] is exposed along the western margin of the range in the footwall of the Las Pirquitas thrust (Figures 2 and 3) and consists of low- to medium-grade quartzite, marble, and less common metavolcaniclastic rocks. On the basis of stratigraphic correlations and detrital zircon ages, the Caucete Group is considered to represent the metamorphosed equivalent of Paleozoic rocks within the Precordillera terrane to the west [e.g., *Ramos et al.*, 1998;

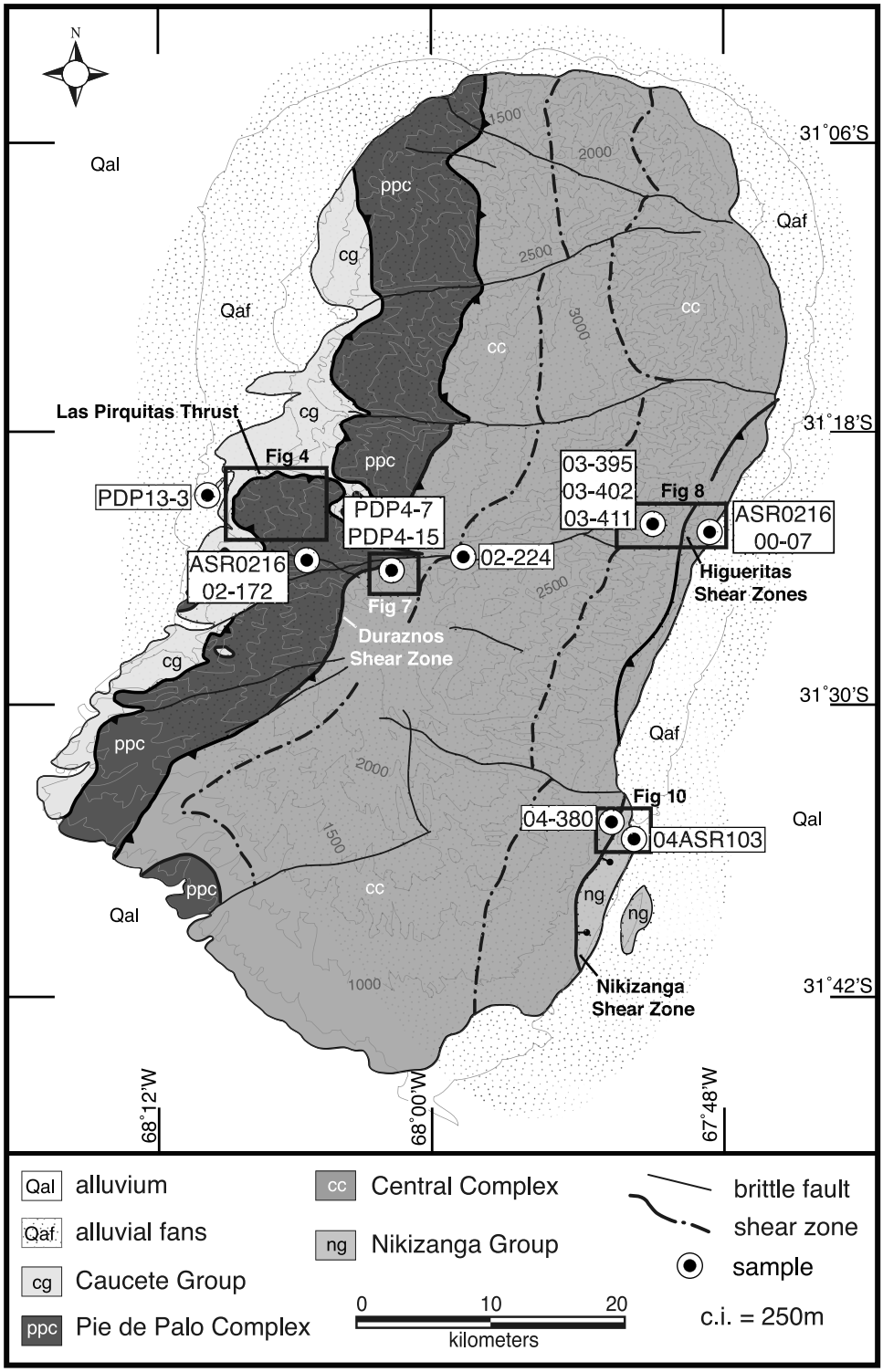

Figure 2. Geologic map of the Sierra de Pie de Palo displaying the first-order structures within range. The locations of more detailed geologic maps are outlined in the black rectangles, and the locations of geochronology samples are shown with circles and sample numbers given in the adjacent white boxes. The map was compiled from regional mapping and published maps [*Dalla Salda and Varela*, 1984; *Ramos et al.*, 1996, 1998; *Casquet et al.*, 2001; *Vujovich et al.*, 2004].

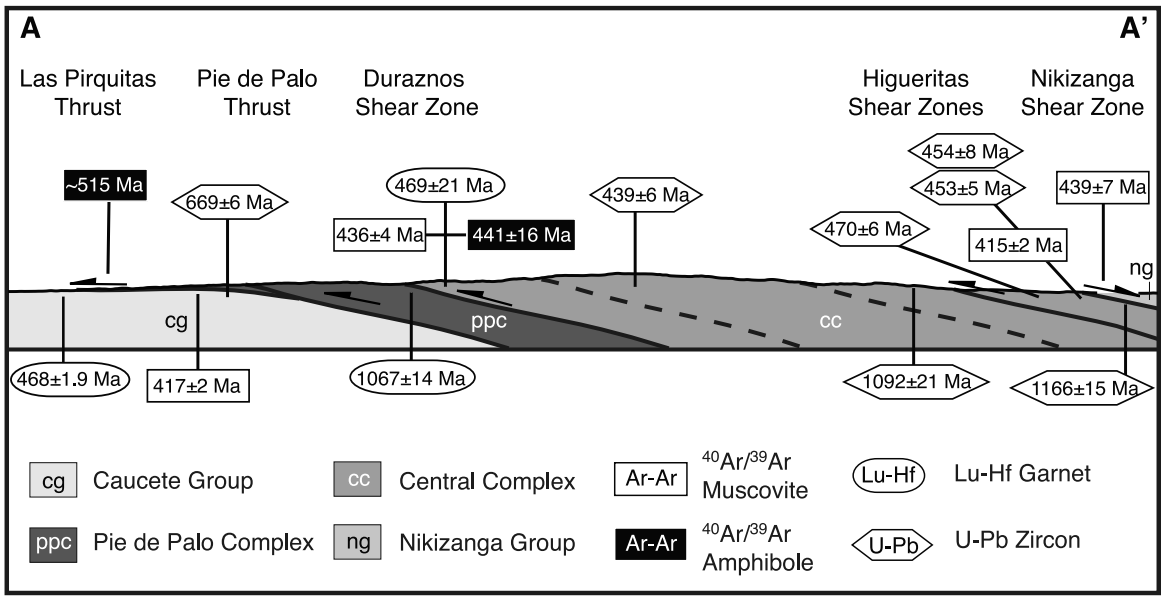

Figure 3. Generalized cross section of the Sierra de Pie de Palo and the locations of U-Pb zircon, Lu-Hf garnet, and $^{40}Ar/^{39}Ar$ amphibole and muscovite geochronology samples from this study and that of *Mulcahy et al.* [2007].

Vujovich and Kay, 1998; *Naipauer et al.*, 2010]. Based on metamorphic mineral assemblages, *Dalla Salda and Varela* [1984] broadly estimated metamorphic conditions of 7 ± 2.5 kbar and 520 ± 70°C for the Caucete Group.

[8] The Pie de Palo Complex occurs along the western margin of the range (Figure 2) and has been described as all of the rocks that lie east of the Las Pirquitas thrust and west of the Nikizanga shear zone [e.g., *Dalla Salda and Varela*, 1984; *Ramos et al.*, 1998; *Vujovich and Kay*, 1998]. Based on our structural mapping and work included in this contribution, we restrict the use of the term Pie de Palo Complex to include only those rocks that lie between the Las Pirquitas thrust and the Duraznos shear zone (Figure 2). We have subdivided the Pie de Palo Complex into three distinct units based on protolith (Figure 4): a mafic and ultramafic unit that consists largely of metagabbro and garnet-amphibolite (ppm), a second unit composed dominantly of intermediate orthogneiss and rare amphibolites (ppo), and a third unit composed of orthogneiss, metatonalite, and metavolcanics (ppt). *Vujovich et al.* [2004] and *Rapela et al.* [2010] obtained Middle Proterozoic U-Pb zircon protolith ages (1204–1110 Ma) from gabbroic pegmatites and dioritic-granodioritic sills within the Pie de Palo Complex. *Vujovich and Kay* [1998] interpreted the mafic and ultramafic rocks of the Pie de Palo Complex to represent an ophiolite sequence formed within a back-arc spreading environment.

[9] We define the Central Complex as the schist, quartzite, metavolcanic, marble, migmatite and amphibolite that occur between the Duraznos and Nikizanga shear zones (Figure 2). This broad classification incorporates the subdivisions of *Dalla Salda and Varela* [1984], *Casquet et al.* [2001], and *Galindo et al.* [2004]. *McDonough et al.* [1993] reported preliminary U-Pb zircon protolith ages of ~938 to ~1091 Ma from orthogneiss across the Central Complex and various authors have reported Cambrian and Ordovician magmatic and metamorphic ages from within the formation [*Varela and Dalla Salda*, 1992; *McDonough et al.*, 1993; *Pankhurst and Rapela*, 1998]. *Casquet et al.* [2001] obtained Ordovician (~460 Ma) peak metamorphic conditions of 13 ± 1 kbar and 600 ± 50°C, followed by decompression during ductile deformation to 9 ± 1.3 kbar and 570 ± 50°C. These authors interpreted the sequence to represent the metamorphosed sedimentary cover to the underlying Pie de Palo Complex [*Casquet et al.*, 2001].

[10] The Nikizanga Group consists of a low- to medium-grade quartzite, marble, graphitic schist, and less abundant amphibolite in the hanging wall of the Nikizanga shear zone in the southeast margin of the range (Figure 2). This unit is recognized on the lower metamorphic grade, lack of significant intrusive rocks, and presence of local pressure solution cleavage in outcrop.

3. Structures Within the Sierra de Pie de Palo

[11] Zones of mylonite and ultramylonite, ranging in scale from decimeters to hundreds of meters, are prevalent throughout much of the Sierra de Pie de Palo, but our research indicates that several first-order shear zones can be defined that bound the major lithotectonic units described above. Below we describe the individual shear zones from west to east.

3.1. The Las Pirquitas and Pie de Palo Thrusts

[12] The western margin of the Sierra de Pie de Palo preserves a complex network of shear zones, the most prominent of which are the Las Pirquitas and Pie de Palo thrusts (Figure 4). We restrict the name Las Pirquitas thrust a low-angle, dominantly east dipping boundary that separates the

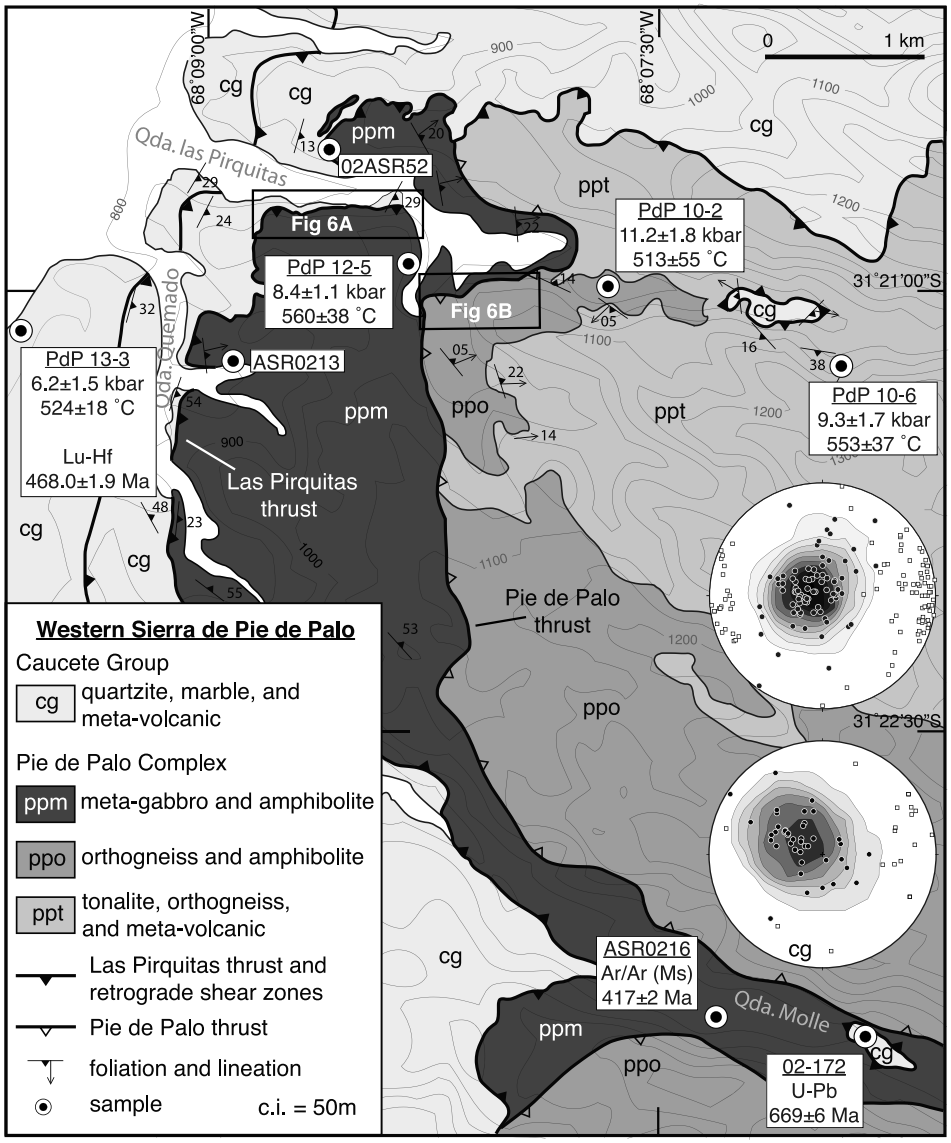

Figure 4. Geologic map of the western Sierra de Pie de Palo in the vicinity of the Las Pirquitas and Pie de Palo thrusts. The location of samples selected for thermobarometry and geochronology are shown. The P-T conditions and ages are listed below the sample numbers: U-Pb zircon age (U-Pb), Lu-Hf garnet age (Lu-Hf), $^{40}Ar/^{39}Ar$ muscovite age (Ar/Ar (Ms)). Inset lower hemisphere, equal area stereoplot shows contoured poles to foliation (solid circles) and stretching lineation (open squares), Pie de Palo Complex (pp) ($n_S = 61$, $n_L = 98$) and Caucete Group (cg) ($n_S = 43$, $n_L = 17$).

Pie de Palo Complex from the underlying Caucete Group (Figures 3 and 4) and is marked by a 2 to 3 m thick retrograde shear zone (Figure 5a). A complex, imbricated shear zone network occurs within the hanging wall of the Las Pirquitas thrust [*Ramos et al.*, 1996] (Figure 6a). The retrograde shear zone truncates the higher-grade mylonitic fabrics developed within the hanging wall, for which *Mulcahy et al.* [2007] obtained $^{40}Ar/^{39}Ar$ hornblende ages of ~515 Ma. The mylonites are overprinted by later events but dominantly display a shallowly dipping foliation, E-W trending mineral lineations (Figure 4) and top-to-the-west kinematic indicators. The Cambrian mylonites are deformed by at least two generations of isoclinal recumbent folds and are locally overprinted by a strong axial planar foliation (Figure 5b). The axial planar fabric becomes a penetrative foliation approaching the Las Pirquitas thrust where it is overprinted by the subparallel retrograde shear zone with a well-defined, top-to-the-west S-C fabric (Figure 5c). The retrograde fabric is itself folded by shallowly plunging NNE-SSW trending folds. The thrust is also exposed as windows east of main thrust exposure [*Ramos et al.*, 1996] (Figure 4) and juxtaposes structurally higher portions of the Pie de Palo Complex against quartzites, carbonates, and metavolcanic rocks interpreted to be the Caucete Group.

[13] The east dipping Pie de Palo thrust occurs within rocks of the Pie de Palo Complex and juxtaposes intermediate

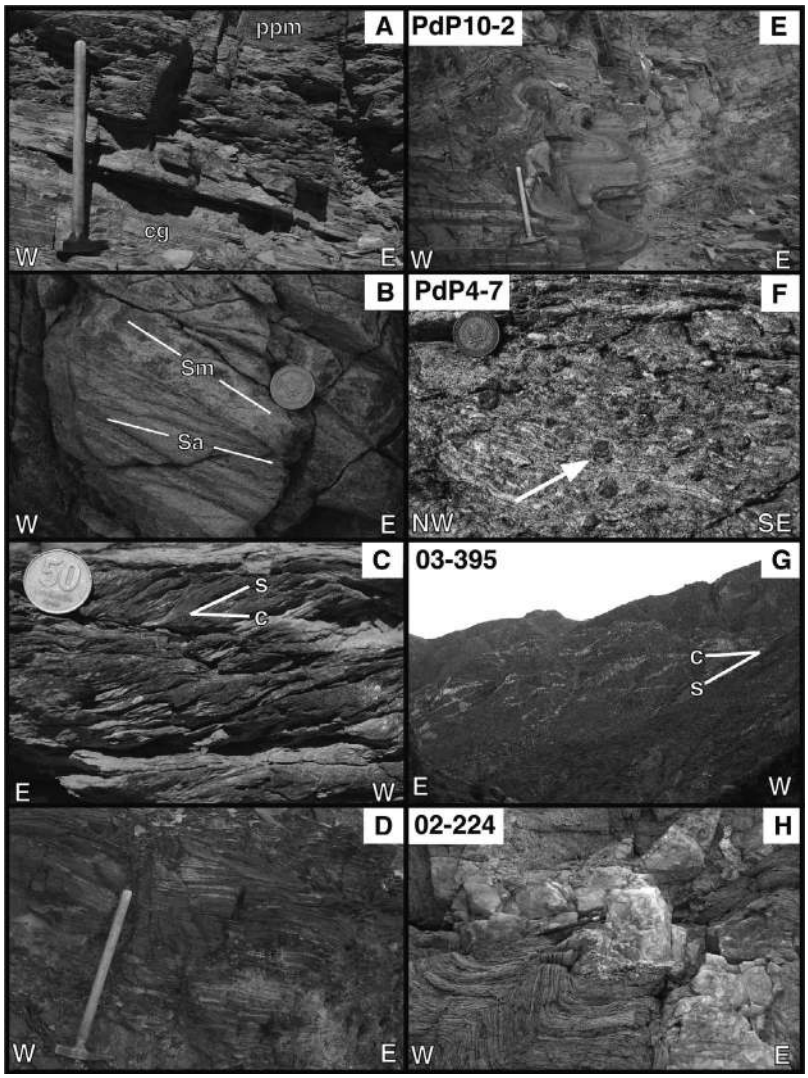

Figure 5. Outcrop photographs from the Sierra de Pie de Palo. (a) Retrograde shear zone of the Las Pirquitas thrust juxtaposes mafic rocks of the Pie de Palo complex (ppm) in the hanging wall against the Caucete Group (cg) in the footwall. (b) Axial planar fabric (Sa) that overprints an older mylonitic foliation (Sm) within the hanging wall of the Las Pirquitas thrust. (c) Top-to-the-west shear fabric within the retrograde shear zone of the Las Pirquitas thrust. (d) Flaggy shear zone fabric of the Pie de Palo thrust that overprints older mylonitic fabrics within the hanging wall. (e) Sample site of PdP10-2 displays isoclinal recumbent folds of mylonitic intermediate orthogneiss within the Pie de Palo Complex. Hammer is 60 cm for scale. (f) Sample PdP4-7, prekinematic garnet porphyroclasts in the hanging wall of the Duraznos shear zone. The arrow points to one garnet with top-to-the-west asymmetric tails of mica and amphibole. (g) Syndeformational granitoids for the western Higueritas shear zone with a top-to-the-west S-C fabric. Sample 03-395 was collected just outside the eastern edge of the photo where the sills intersect the base of the wash. (h) Sample 02-224, K-feldspar pegmatitic dike that cuts north trending folds within the Central Complex.

composition orthogneiss, amphibolite, and metavolcanic rocks in the hanging wall against more mafic metagabbros and garnet amphibolites in the footwall (Figures 4 and 6b). The shear zone is marked by a 3 to 4 m thick zone of flaggy mylonite (Figure 5d) that overprints an older, isoclinal recumbently folded mylonitic fabric in the hanging wall (Figure 5e). The mylonitic foliation is shallowly dipping and kinematic indicators indicate top-to-the-west sense of motion. The Pie de Palo thrust is part of the complexly imbricated shear zone network within the Pie de Palo Complex (Figure 6b).

3.2. The Duraznos Shear Zone

[14] The east dipping Duraznos shear zone (Figures 2 and 3) is a ~600 m wide mylonite zone that juxtaposes metasediments, metavolcanic rock, and orthogneiss in the hanging wall against metamorphosed mafic and ultramafic

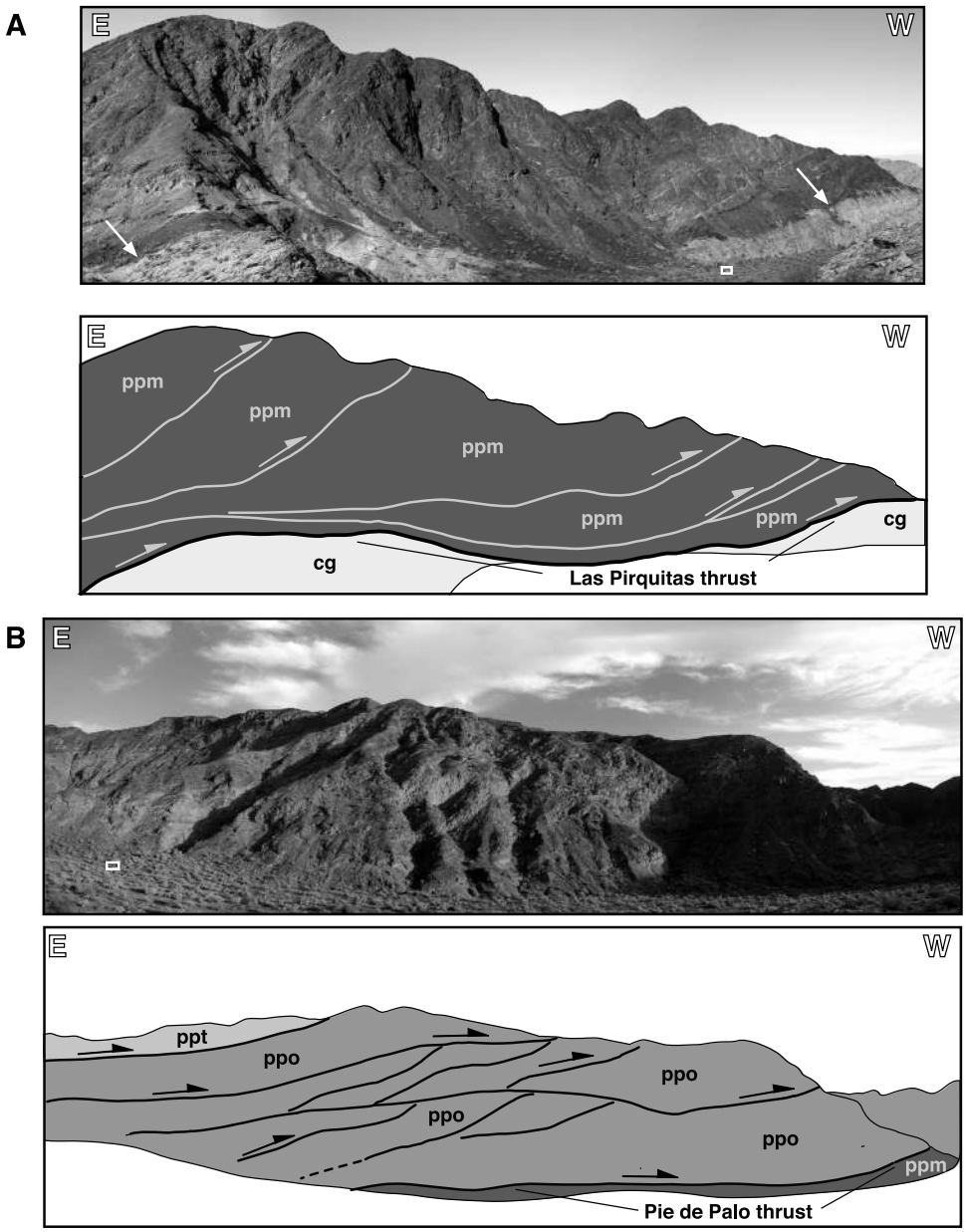

Figure 6. Photographs and interpretive diagrams of imbricate top-to-the-west thrusts that comprise (a) the Las Pirquitas thrust and (b) the Pie de Palo thrust. Both duplex systems deform older generations of mylonitic shear zones that have been folded by at least two generations of isoclinal recumbent folds. The photographs were taken in Quebrada Las Pirquitas (Figure 3) and are viewed toward the south. The white rectangle in each photograph outlines a 4 × 4 pickup for scale. The arrows in Figure 6a mark the main trace of the retrograde Las Pirquitas thrust, which separates the Pie de Palo complex in the hanging wall from the Caucete group in the footwall. All unit labels are as in Figure 4.

intrusive and metavolcanic rock of the Pie de Palo Complex in the footwall (Figure 7). The mylonitic fabric strikes northeast to southwest, dips moderately to the southeast, and is truncated in the northeast by the subvertical Molle brittle fault (Figure 7). In both the footwall and hanging wall, the fabric intensity increases gradually toward the Duraznos shear zone. The transition is well exposed and unlike the zone between the Las Pirquitas and Pie de Palo thrusts, no breaks exist in the structural section due to late stage faulting. The mean mineral lineation, defined by aligned amphibole, mica, and stretched quartz, has a rake of ~45° to the average strike of the mylonitic fabric (Figure 7). Asymmetric tails on garnet (Figure 5f), plagioclase, kyanite, and staurolite porphyroclasts, and mica fish indicate top-to-the-west sense of motion along the shear zone. The oblique rake is consistently to the north of the dip-slip component indicating a dextral

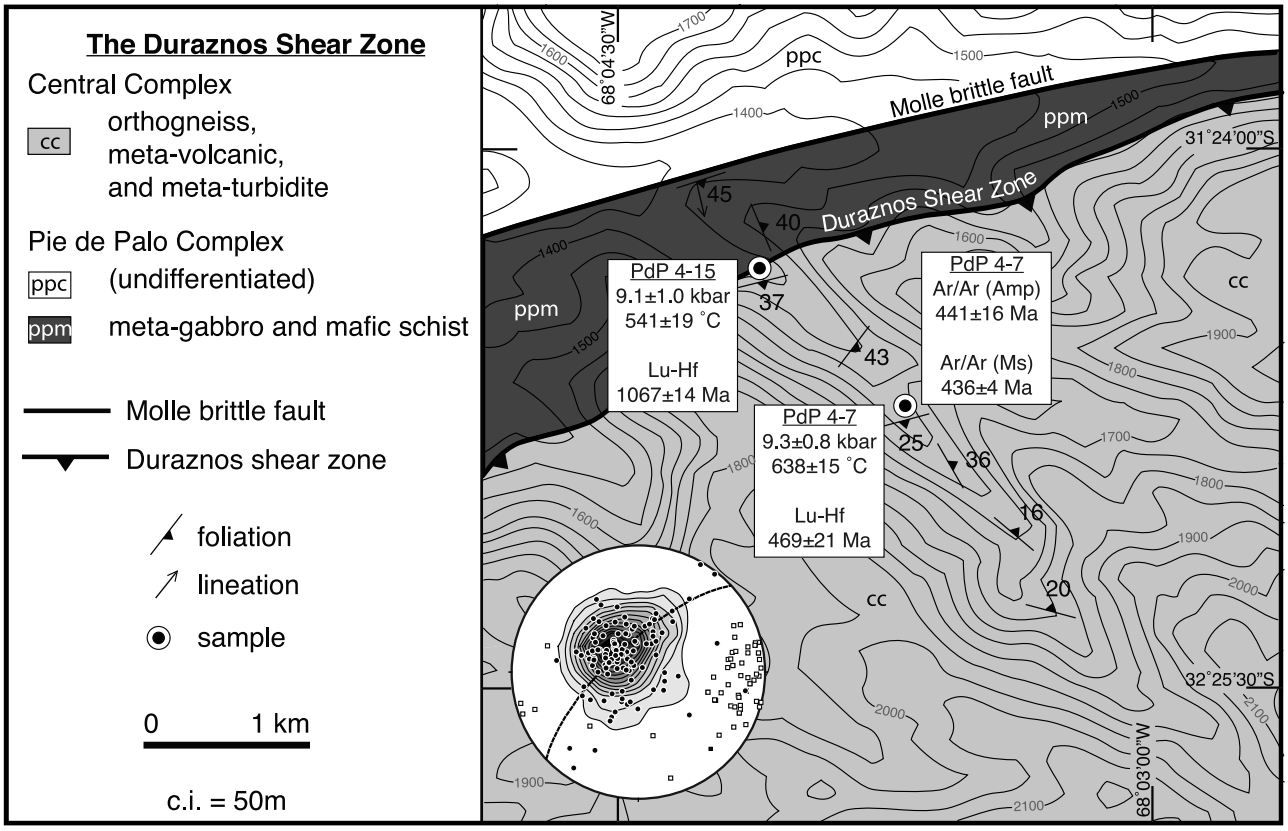

Figure 7. Geologic map of the Duraznos shear zone. The P-T conditions and ages for samples PdP4-15 from the footwall of the Duraznos shear zone and PdP4-7 from the hanging wall are listed below the sample numbers: Lu-Hf garnet age (Lu-Hf), $^{40}Ar/^{39}Ar$ amphibole age (Ar/Ar (Amp)), $^{40}Ar/^{39}Ar$ muscovite age (Ar/Ar (Ms)). Inset lower hemisphere, equal area stereoplot shows contoured poles to foliation (solid circles, $n_S = 170$) and stretching lineation (open squares, $n_L = 64$).

component of slip. Away from the shear zone fabric in the hanging wall, recumbent isoclinal folds deform the metasediment and metavolcanic rocks. Small-scale granitic intrusives locally cross cut and intrude fold hinges.

3.3. The Higueritas Shear Zones

[15] Several east dipping shear zones occur within Quebrada Higueritas along the eastern margin of the Sierra de Pie de Palo (Figures 2 and 8). Granitic bodies, ranging in thickness from centimeter to meter scale, appear throughout the canyon and occur as: undeformed dikes that cross cut the mylonitic fabrics, as variably folded sills that are deformed by the mylonitic fabrics, and as dikes and sills that preserve an igneous fabric within their interior but that share a mylonitic fabric with the country rock along their margins.

[16] The western Higueritas shear zone has a structural thickness of ~600 to 800 m and occurs within the quartzite, orthogneiss, and amphibolite within the footwall of the eastern Higueritas shear zone (Figure 8). No obvious change in protolith occurs across this boundary but a discontinuous horizon of granitic sills defines an S-C geometry (Figure 5g) and occurs at the upper boundary of the shear zone. Similar to the Duraznos shear zone, the mean mineral lineation, defined by aligned amphibole, mica, and stretched quartz, has a rake of ~55° to the average strike of the mylonitic fabric (Figure 8). Kinematic indicators within the shear zone mylonites and the S-C fabric within the granitoids (Figure 5g) are consistent with top-to-the-west thrusting. Similar to the Duraznos shear zone, the oblique rake is consistently to the north of the dip-slip component indicating a dextral component of slip.

[17] The eastern Higueritas shear zone (Figure 8) is a ~750 to 1000 m thick mylonite zone that juxtaposes quartzite and carbonate in the hanging wall against quartzite, orthogneiss, and less common amphibolite in the footwall. Kinematic indicators within the shear zone, such as asymmetric tails on garnet porphyroblasts and plagioclase porphyroclasts dominantly display a top-to-the-west sense of motion. Fabric intensity related to the shear zone decreases structurally upsection from the base of the shear zone. Well-developed quartzo-feldspathic mylonites along the range front exhibit local top-to-the-east kinematics (Figures 8 and 9a).

3.4. The Nikizanga Shear Zone

[18] The east dipping Nikizanga shear zone is exposed along the southeastern margin of the Sierra de Pie de Palo (Figure 2). The region exhibits a moderate to shallowly southeast dipping foliation and an east plunging lineation (Figure 10). The shear zone juxtaposes low- to medium-

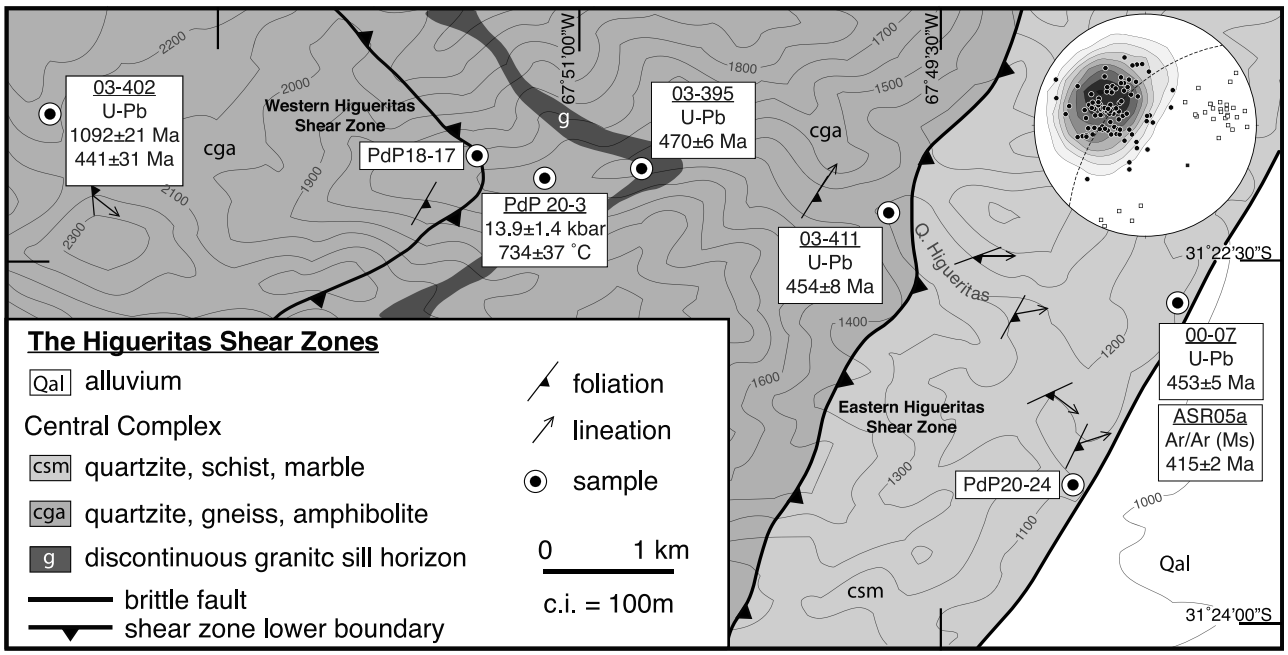

Figure 8. Geologic map of the Higueritas shear zone. The PT conditions and ages are listed below the sample numbers: U-Pb zircon age (U-Pb), $^{40}Ar/^{39}Ar$ muscovite age (Ar/Ar (Ms)). Inset lower hemisphere, equal area stereoplot shows contoured poles to foliation (solid circles, $n_S = 48$) and stretching lineation (open squares, $n_L = 36$).

grade quartzite, marble, and graphitic schist in the hanging wall against orthogneiss, migmatite, schist, and granitoid in the footwall. The hanging wall rocks locally exhibit a strong pressure solution cleavage and lack granitic rocks, in contrast to the footwall. In outcrop, asymmetric tails on garnet indicate top-to-the-southeast sense of motion on the shear zone.

4. Petrology and Thermobarometry

[19] We selected samples from across the structural transect to compare the metamorphic conditions of the various units and to assess if any breaks in pressure and/or temperature occur between major structures (Table 1). Mineral compositions were determined by electron probe microanalysis using a Cameca SX-100 at UC, Davis. Natural and synthetic materials were used as standards. An accelerating voltage of 15 kV was used for all analyses, a 1 μm beam was used for garnet, amphibole, and epidote, and 10 μm beam was used for analyses of plagioclase, chlorite, muscovite, and biotite. Mineral compositions are provided in the auxiliary material.[1] Pressure and temperature conditions were estimated by the average P-T method [*Powell and Holland*, 1994] using the software THERMOCALC (v3.25). Mineral activities were calculated with the accompanying software AX.

[20] Within the footwall of the Las Pirquitas thrust, the La Paz member of the Caucete Group contains Grt-Chl-Ep-Pl-Hbl-Qtz schist (mineral abbreviations after *Kretz* [1983]) and is interpreted as a metavolcanic horizon. The greenschist facies assemblage preserves a single generation of small (<0.5 mm) euhedral garnet (Figure 11a) that displays Sps-rich and Alm-poor cores that decrease and increase, respectively, toward the rim (Figure 12a), suggestive of one phase of prograde growth zoning. The sample records P-T conditions of 6.2 ± 1.5 kbar and 524 ± 18°C.

[21] Within the hanging walls of the Las Pirquitas and Pie de Palo thrusts, mafic and intermediate units commonly preserve evidence of two distinct generations of garnet. Garnet amphibolite from the lower member of the Pie de Palo Complex (ppm) displays thin, distinct rims on large poikilitic garnet (Figure 11b). End-member composition profiles across the core to rim (Figure 12b) show elevated Alm and lower Grs in the core of the garnet with respect to the rim. Four samples were selected for thermobarometry within the Pie de Palo Complex and show no discernible breaks in P-T conditions across the imbricate network of shear zones associated with the Las Pirquitas and Pie de Palo thrusts. Using garnet rims and matrix mineral compositions, all four samples are consistent with weighted average P-T conditions of 9.1 ± 1.5 kbar and 544 ± 15°C for the latest stage of metamorphism.

[22] Within the footwall of the Duraznos shear zone, Hbl-Grt-Pl-Qtz ± Rt-Ilm-Chl-Cal metavolcanic rocks preserve two distinct generations of garnet. Large (~2 mm) garnets are wrapped by the mylonitic foliation and contain optically distinct cores with euhedral faces (Figure 11c). The second generation occurs as distinct rims on large garnets and as fine garnets within the matrix that locally cross cut the mylonitic foliation (Figure 11d). Large garnet cores show little to no zoning (Figure 12c). The rims are compositionally similar to fine matrix garnet, which display elevated Sps and Grs in the cores and Pyr and Alm increasing toward the rims, suggesting

[1] Auxiliary materials are available at ftp://ftp.agu.org/apend/tc/2009tc002656.

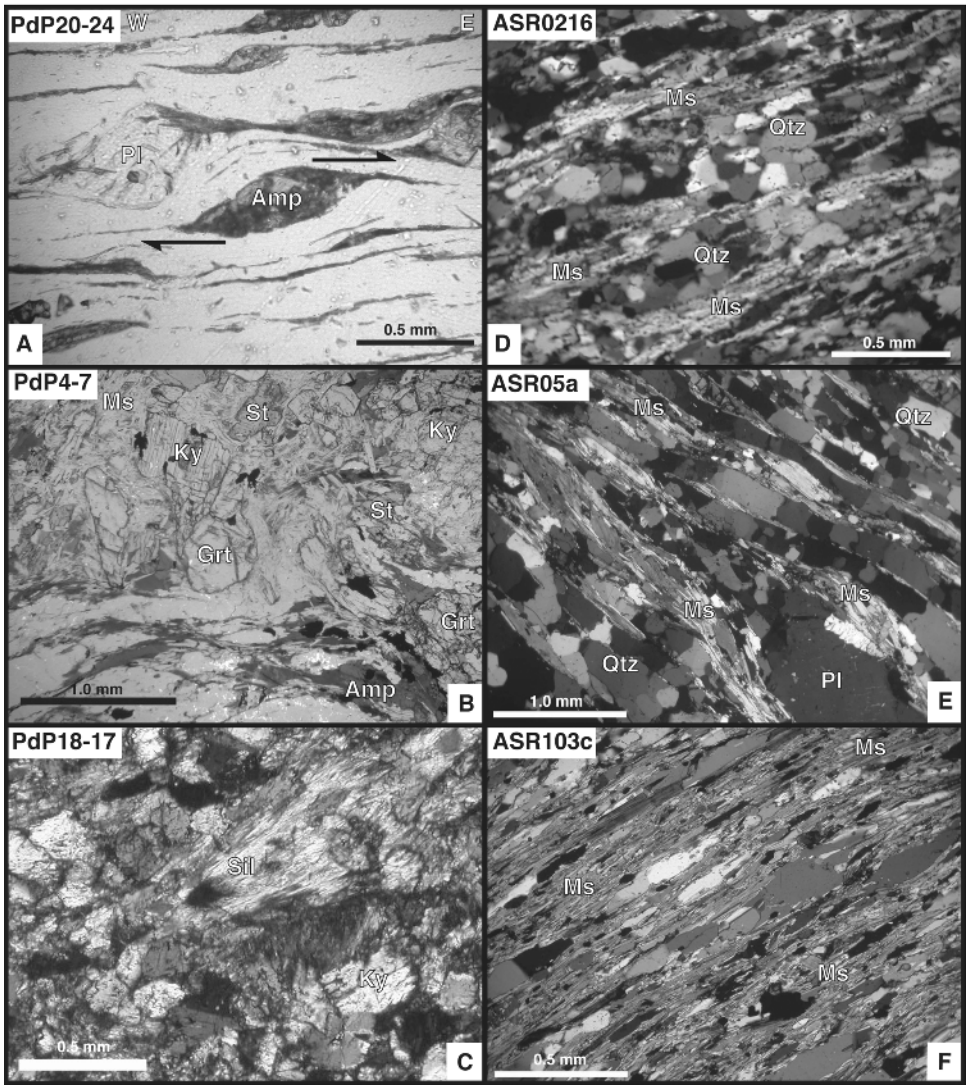

Figure 9. Photomicrographs from samples within the Sierra de Pie de Palo. (a) Amphibole (Amp) and plagioclase (Pl) sigma porphyroclasts with top-to-the-west asymmetry from the Higueritas shear zone. (b) Kyanite (Ky), staurolite (St), and garnet (Grt) rimmed by muscovite (Ms) and amphibole (Amp) from sample PdP4-7 in the hanging wall of the Duraznos shear zone. (c) Twinned kyanite (Ky) replaced by fibrous sillimanite (Sil) from near the granitoid horizon in the Higueritas shear zone. (d) Quartz-rich Ms-Pl-Ep schist from the western Caucete Group window exposed in Quebrada Molle ($^{40}Ar/^{39}Ar$ muscovite sample ASR0216). (e) Muscovite schist from the eastern range front in the hanging wall of the Higueritas shear zone ($^{40}Ar/^{39}Ar$ muscovite sample ASR05a). Muscovite (Ms) wraps plagioclase porphyroclasts (Pl) and defines the foliation with alternating quartz-rich horizons (Qtz). (f) Muscovite schist from the hanging wall of the Nikizanga shear zone ($^{40}Ar/^{39}Ar$ muscovite sample ASR103c).

prograde growth zoning (Figure 12d). Postkinematic prograde garnet growth suggests that heating outlasted deformation within the footwall. The matrix mineral assemblage combined with garnet overgrowths resulted in P-T conditions of 9.1 ± 1.0 kbar and 549 ± 19°C.

[23] Hanging wall rocks of the Duraznos shear zone contain the assemblage Grt-Bt-Ms-Qtz-Pl ± Ky-St-Hbl-Ep-Rt-Ilm. Inclusions of Qtz-St-Pl-Ms-Bt-Ky, within large (~2.5 mm) garnets define a straight internal foliation aligned at high angle to the mylonitic fabric (Figure 11e) suggesting that the main episode of garnet growth was prekinematic. Compositionally distinct overgrowths locally occur along the rims of uniform core compositions that are elevated in Grs and Pyr and depleted in Sps with respect to the main phase of garnet (Figure 12e). The garnet profile suggests diffusional zoning of prekinematic garnet as a result of cooling from high temperatures followed by a second phase of garnet growth during the mylonitic event. The hanging wall assemblage records P-T conditions of 9.3 ± 0.8 kbar and 638 ± 15°C.

[24] Rocks within the western Higueritas shear zone contain the assemblage Grt-Bt-Ms-Pl-Qtz ± Kfs ± Ky ± Sil.

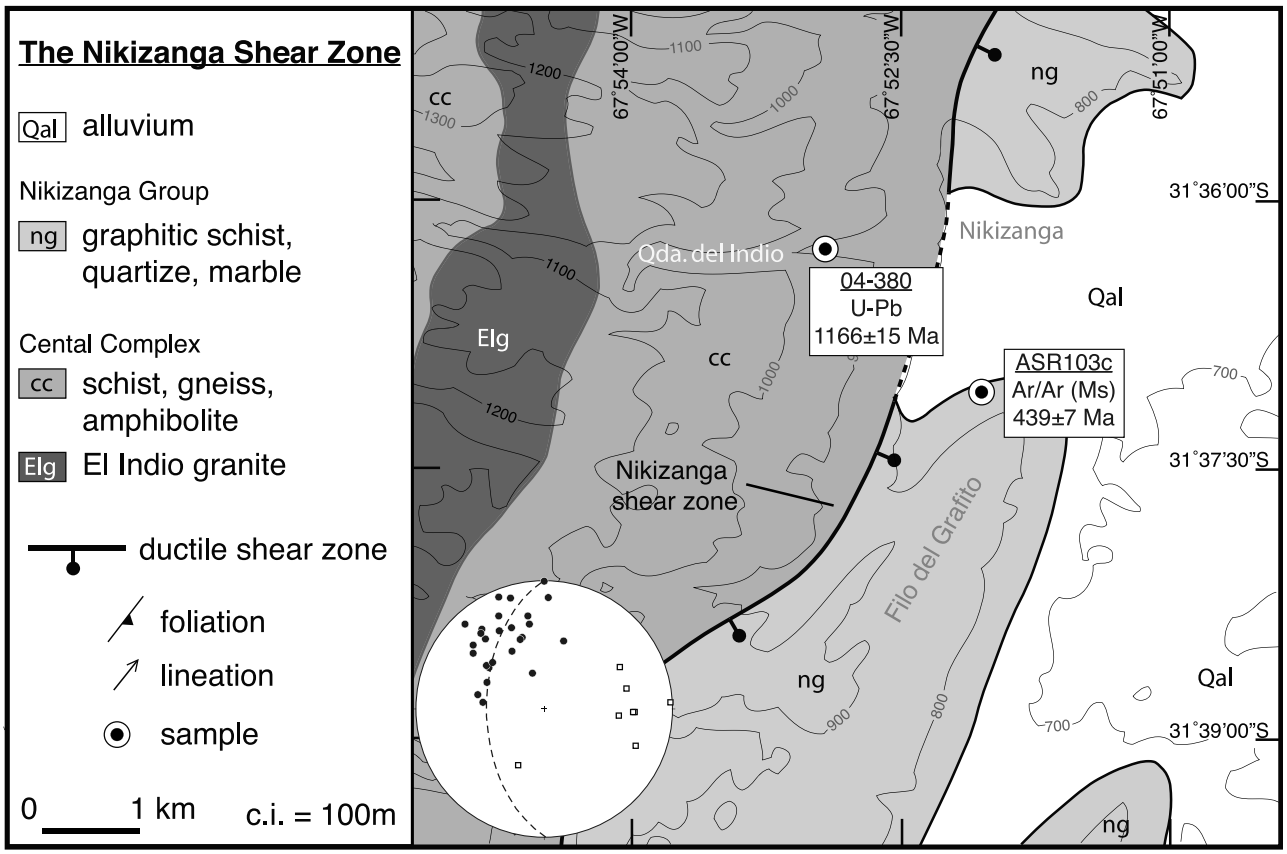

Figure 10. Geologic map of the Nikizanga shear zone along the eastern margin of the Sierra de Pie de Palo. The ages are listed below the sample numbers: U-Pb zircon age (U-Pb), $^{40}Ar/^{39}Ar$ muscovite age (Ar/Ar (Ms)). Inset lower hemisphere, equal area stereoplot shows contoured poles to foliation (solid circles, $n_S = 26$) and stretching lineation (open squares, $n_L = 8$).

Euhedral garnet displays prograde growth zoning with elevated Sps and Grs in the cores and Pyr and Alm increasing toward the rim (Figure 12f). Locally, sillimanite replaces kyanite (Figure 9c), grows as top-to-the-west tails on asymmetric kyanite porphyroclasts, occurs within the mylonitic foliation wrapping garnet and plagioclase, and locally grows radially across the mylonitic fabric. These observations suggest that sillimanite grew during and after top-to-the-west thrusting along the western Higueritas shear zone. The observations imply heating and/or decompression from the kyanite to sillimanite stability field during and after deformation. Pressure-temperature conditions from aluminosilicate free Grt-Bt-Ms-Qtz-Pl orthogneiss records conditions of 13.9 ± 1.4 kbar and 734 ± 37°C.

[25] The majority of the first-order structures record discernible breaks in pressure and/or temperature (Figures 13a

Table 1. THERMOCALC Average Pressure-Temperature Results From Samples Selected for This Study[a]

Sample	Location	Lithology	Pressure (kbar) ± 2σ	Temperature (°C) ± 2σ	σ_{fit}[b]	Phases
			Caucete Group			
PdP13-3	Figure 4	metavolcanic	6.2 ± 1.5	524 ± 18	1.29 (1.45)	Grt, Amp, Bt, Pl, Chl, Ep, Qtz, H_2O
			Pie de Palo Complex			
PdP12-5	Figure 4	metagabbro	8.4 ± 1.1	560 ± 38	1.05 (1.54)	Grt, Amp, Pl, Ep, Qtz, H_2O
PdP10-2	Figure 4	orthogneiss	11.2 ± 1.9	513 ± 55	1.43 (1.49)	Grt, Amp, Bt, Pl, Ep, Qtz, H_2O
PdP10-6	Figure 4	metavolcanic	9.3 ± 1.7	553 ± 37	0.58 (1.73)	Grt, Pl, Ep, Qtz, H_2O
PdP4-15	Figure 7	metavolcanic	9.1 ± 1.0	549 ± 19	1.89 (1.45)	Grt, Amp, Chl, Ep, Qtz, H_2O
			Central Complex			
PdP4-7	Figure 7	metavolcanic	9.3 ± 0.8	638 ± 15	1.31 (1.35)	Grt, Amp, Bt, Pl, Ep, St, Ky, Qtz, H_2O
PdP20-3	Figure 8	orthogneiss	13.9 ± 1.4	734 ± 37	1.40 (1.61)	Grt, Bt, Ms, Pl, Qtz, H_2O

[a]All samples passed σ_{fit} equal to or less than the maximum value predicted by the assemblage [*Powell and Holland*, 1994].
[b]Values in parentheses are the minimum σ_{fit} value acceptable for the mineral assemblage used in the calculation.

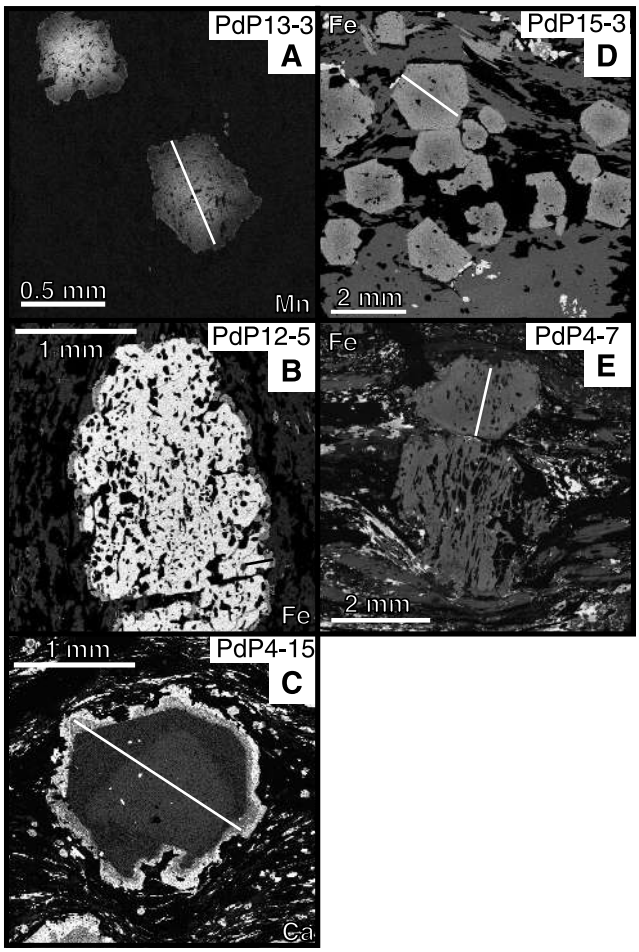

Figure 11. Elemental WDS maps showing compositional zoning in garnets from the Sierra de Pie de Palo. The solid lines on the garnet in each of the images mark the location of composition profiles shown in Figure 12. (a) Sample PdP13-3, a metavolcanic from the La Paz member of the Caucete Group (Figure 4). (b) Sample PdP12-5, a metagabbro from the Pie de Palo Complex in the footwall of the Pie de Palo thrust (Figure 4). (c) Samples PdP4-15, a metavolcanic, and (d) PdP15-1, a metagabbro, are from the Pie de Palo Complex in the footwall of the Duraznos shear zone (Figure 7). (e) Sample PdP4-7, a metavolcanic from the Central Complex in the hanging wall of the Duraznos shear zone (Figure 7). Note the straight internal foliation within garnet at a high angle to the external mylonitic foliation.

and 13b). Across the Las Pirquitas thrust, the Caucete Group was metamorphosed at considerably lower pressure (~6 kbar) than the Pie de Palo Complex (~9 kbar) (Figure 13a) yet there is no discernible break in temperature across the thrust (Figure 13b). Within the Pie de Palo complex, however, variably deformed units record equivalent P-T conditions of 9.1 ± 1.5 kbar and 544 ± 15°C. Pressure remains constant across the Duraznos shear zone but distinctly different temperatures are recorded in the footwall (~540°C) and hanging wall (~638°C) (Figure 13b). The pressure and temperature conditions in the hanging wall of the Higueritas shear zone (13.9 ± 1.4 kbar and 734 ± 37°C) are greater than in the hanging wall of the Duraznos shear zone (Figure 13). Our structural transect between the two shear zones is not detailed enough to exclude the presence of other major shear zones. *Casquet et al.* [2001], however, report premylonitic conditions of 13 ± 1 kbar and 600 ± 50°C within the hanging wall of what we have defined as the Duraznos shear zone that are broadly equivalent to pressure-temperature conditions within the Higueritas region. The younger Duraznos shear zone may therefore overprint fabrics related to the Higueritas shear zone, requiring ~4 kbar of exhumation between the two events.

5. Geochronology

[26] Our structural mapping and thermobarometry indicate that the Sierra Pie de Palo preserves a series of individual lithotectonic units separated by discrete shear zones. In order to determine the protolith age of the individual thrust sheets and the timing and extent of magmatism, metamorphism, and deformation we have conducted U-Pb zircon geochronology, Lu-Hf garnet geochronology, and $^{40}Ar/^{39}Ar$ thermochronology from selected samples across the range. The ages determined for each sample are summarized in Table 2.

5.1. U-Pb Geochronology

[27] We collected samples of deformed intrusive and metavolcanic rocks throughout the range in order to constrain both the timing of deformation on major structures and the protolith age of units within the Sierra de Pie de Palo. All samples were analyzed using the SHRIMP-RG at the USGS–Stanford University ion probe laboratory. Analytical data are provided in the auxiliary material.

[28] Sample 02-172 is a metadacite/rhyolite exposed in the easternmost Caucete window in Quebrada Molle (Figure 4). The unit occurs at the top of the exposed Caucete Group within the window. Rounded grains yielded ages between ~1200 Ma to ~1020 Ma whereas euhedral grains yielded late Proterozoic ages that trail down to ~570 Ma (Figure 14a). Seven analyses of zircon cores give a concordia age of 669 ± 6 Ma (mean square weighted deviation, MSWD = 1.5) that we interpret as the crystallization/deposition age of the metadacite/rhyolite.

[29] Sample 02-224 is a pegmatitic leucogranite dike that cross cuts a fold in the center of the range (Figures 2 and 5h). The eighteen analyzed grains range in age from ~1100 Ma to ~410 Ma (Figure 14b); the older grains are interpreted as inherited components and the younger grains we interpret to record the crystallization age of the leucogranite. Planar regression of all the analyses, assuming a single inheritance age, yielded intercepts of 1118 ± 110 Ma and 463 ± 85 Ma. We rejected the majority of analyses on the basis of obvious or probable inheritance and Pb loss. Four of the eighteen analyses resulted in a concordia age of 439 ± 6 Ma (MSWD = 1.4) that we interpret as the age of crystallization.

[30] Sample 03-402 is metavolcanic/volcaniclastic sample from within the Central Complex (Figure 8). Zircons display oscillatory or sector zoned cores overgrown by thick oscillatory-zoned rims. One rim yielded a Paleozoic age (~436 Ma) that we interpret as a metamorphic age based on a

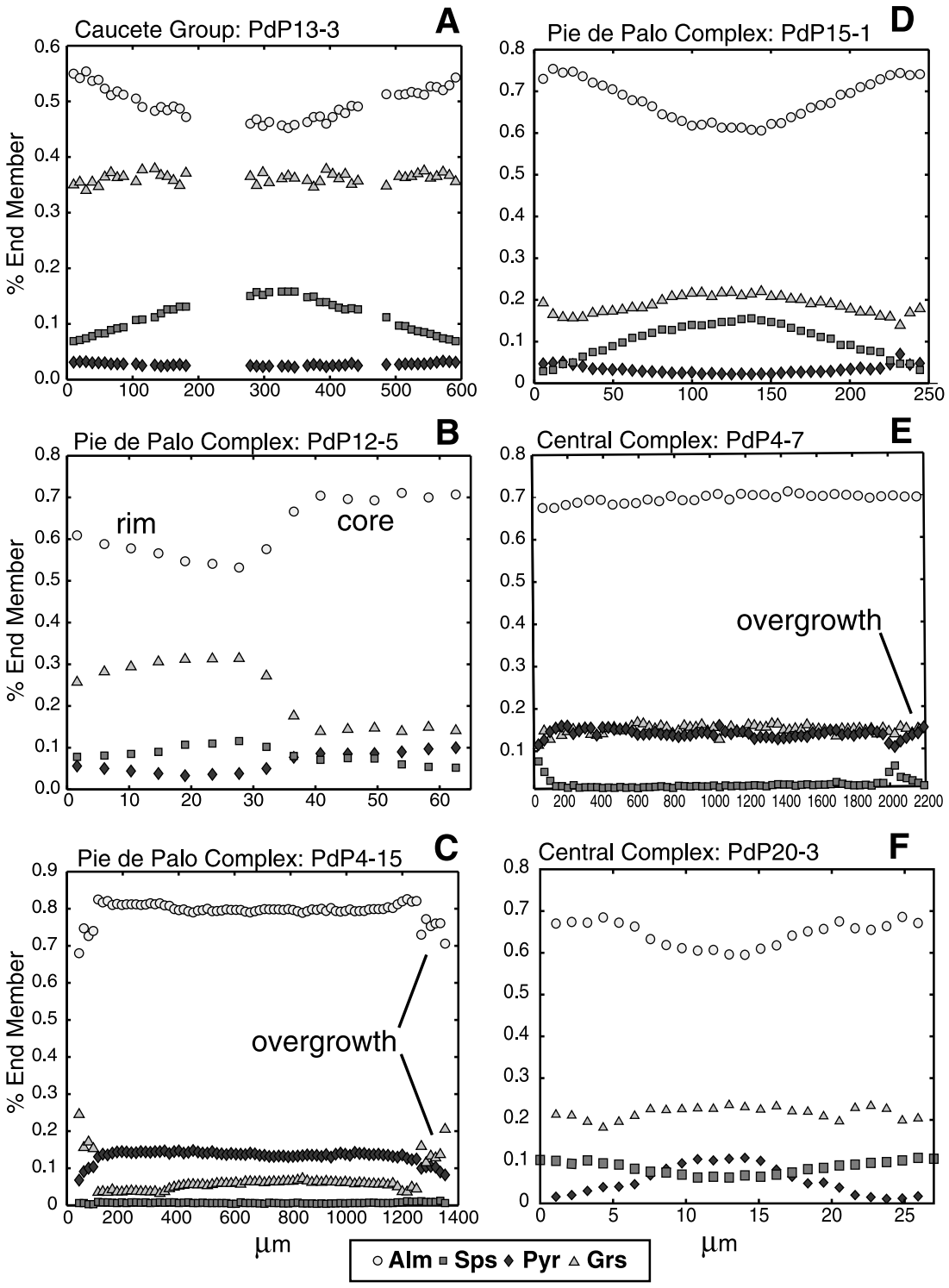

Figure 12. End-member composition traverse profiles of garnets from the Sierra de Pie de Palo. (a) Rare garnet from metavolcanic members of the Caucete Group contains garnets with distinct prograde growth zoning. (b) Garnets form the Pie de Palo Complex characteristically display distinct overgrowths on the rims of older garnet. (c) The footwall of the Duraznos shear zone has relatively unzoned cores with distinct overgrowths. (d) Small, posttectonic garnets in the footwall of the Duraznos shear zone show prograde growth zoning and compositions similar to distinct overgrowths on older garnet. (e) Large garnets from the hanging wall of the Duraznos shear zone and (f) garnet profile from the western Higueritas shear zone.

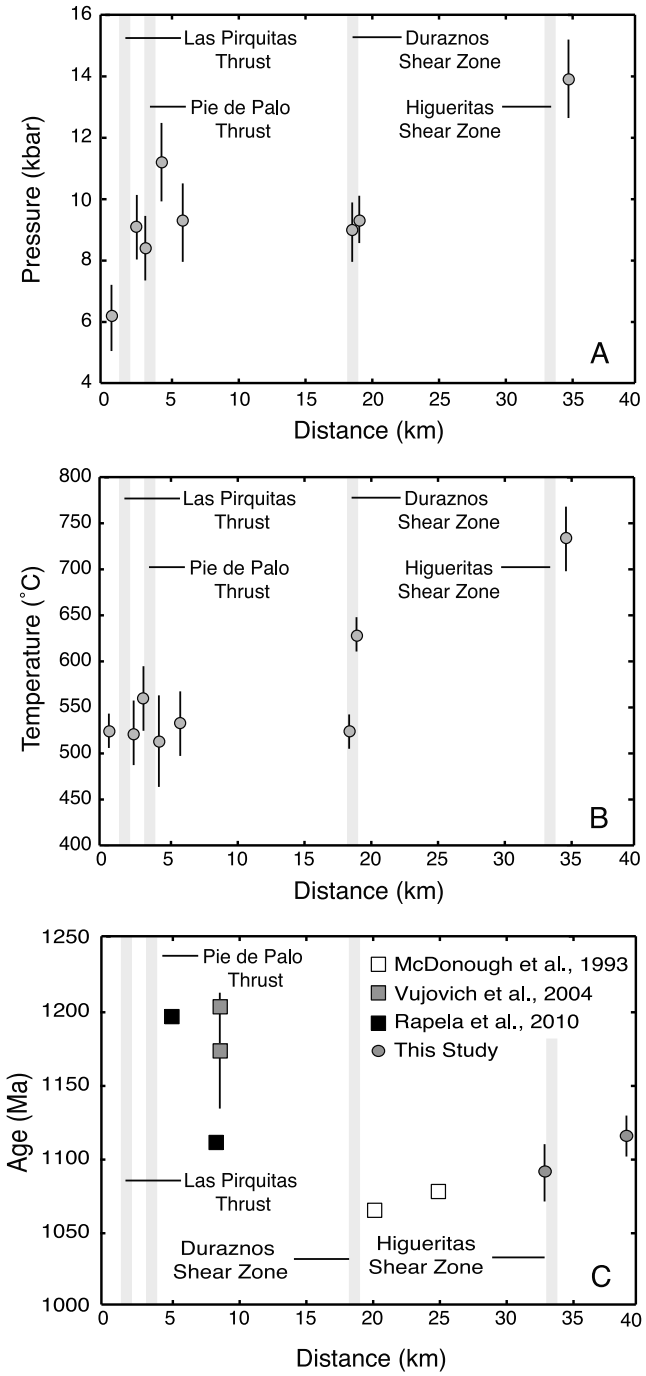

Figure 13. (a) Pressure, (b) temperature, and (c) zircon U-Pb ages of orthogneiss bodies within the Pie de Palo Complex and Central Complex as a function of distance along the cross-section line. Error bars for all analyses are shown at the two-sigma level. The locations of major structures are depicted as vertical grey bars.

distinctly lower Th/U ratio of 0.03. Excluding one analysis containing high common Pb and another older core interpreted as inheritance, linear regression of the remaining core and rim analyses yielded an upper intercept of 1092 ± 21 Ma and a lower intercept of 441 ± 31 Ma (MSWD = 1.5) (Figure 14c), which we interpret as the timing of crystallization and later metamorphism, respectively.

[31] Sample 03-395 was collected from granitic sills whose geometry define an S-C fabric within the western Higueritas shear zone (Figures 8 and 5g) and that we interpret as syn-kinematic with respect to this episode of deformation. Analyses of oscillatory zircon spread from ~470 Ma toward ~400 Ma and show no discernible difference between core and rim ages (Figure 14d). We interpret the younger analyses to have resulted from Pb loss. Nine of nineteen core and rim analyses define a concordia age of 470 ± 6 Ma (MSWD = 1.0), which we interpret as the crystallization age.

[32] Sample 03-411 is a weakly foliated granodiorite sill within the Central Complex (Figure 8). The sample contains oscillatory zoned zircons overgrown by zoned rims, however analyses of the rims was complicated by high amounts of common Pb. Seven of nineteen analyses of zircon cores define a concordia age of 454 ± 8 Ma (MSWD = 1.5) (Figure 14e), which we interpret as the crystallization age.

[33] Sample 00-07 is a penetratively foliated granitic sill exposed on the eastern margin of the Sierra de Pie de Palo (Figure 8). Two grains contained Proterozoic cores, interpreted as inheritance. Twelve analyses yielded a concordia age of 453 ± 5 Ma (MSWD = 1.4) (Figure 14f) that we interpret as the crystallization age.

[34] Sample 04-380 is a foliated orthogneiss in the footwall of the Nikizanga shear zone (Figure 10). Three rim analyses spread to younger $^{207}Pb/^{206}Pb$ ages and are interpreted to record Pb loss and one older core analysis is interpreted as inherited (Figure 14g). Four mutually overlapping analyses of cores and rims provide a concordia age of 1166 ± 15 Ma, that we interpret as the age of crystallization.

[35] The Late Proterozoic age of 669 Ma of metadacite/rhyolite exposed in Querada Molle (Figure 4) is the youngest protolith age determined in this study and, if correlative with the Caucete Group, constrains deposition of at least part of the Caucete Group to ≥669 Ma. This age is distinctly older than the Middle–Late Cambrian age inferred by *Galindo et al.* [2004] on the basis of $^{87}Sr/^{86}Sr$ isotopes from metacarbonates and from detrital zircon ages in quartzites of the Caucete Group [*Naipauer et al.*, 2010]. The discrepancy implies that either older, unrecognized units exist within the Caucete Group or units exposed within the structural windows are not correlative with the Caucete Group.

[36] The new and existing U-Pb ages indicate that discrete shear zones juxtapose rocks of different protolith and metamorphic ages, consistent with the breaks in metamorphic conditions across major structures. *Vujovich et al.* [2004] and *Rapela et al.* [2010] documented U-Pb zircon ages from metamorphosed gabbro, diorite, and granodiorite within the Pie de Palo Complex of ~1110–1200 Ma. In contrast, *McDonough et al.* [1993] report preliminary ages of ~1060 Ma and ~1079 Ma from the Central Complex in an extended abstract, however, additional supporting details were not published and it is possible that some of the ages may be metamorphic [e.g., *Rapela et al.*, 2010]. The former data are plotted with our results along a west to east transect across the Sierra (parallel to the cross section in Figure 3) and are shown in Figure 13c. Though only a few ages, the data

Table 2. Summary of Geochronology Presented in the Text

Sample	Location	Coordinates (Lat., Long.)	Unit	Age (Ma)	MSWD	Comments
				U-Pb Zircon		
02-172	Figure 4	31°23′47.60″S, 68°06′22.82″W	Caucete Group	669 ± 6	1.5	Crystallization/deposition age of metadacite/rhyolite.
02-224	Figure 2	31°23′46.93″S, 68°05′19.13″W	Central Complex	439 ± 6	1.4	Lower intercept crystallization age of pegamititic leucogranite.
03-402	Figure 8	31°21′55.11″S, 67°53′15.91″W	Central Complex	441 ± 31	1.5	Lower intercept metamorphic age of Proterozoic meta-volcanic.
03-395	Figure 8	31°22′23.38″S, 67°51′08.20″W	Central Complex	470 ± 6	1.0	Crystallization age of synkinematic S-C granitoid
03-411	Figure 8	31°22′15.48″S, 67°49′41.27″W	Central Complex	454 ± 8	1.5	Crystallization age of foliated granodiorite
00-07	Figure 8		Central Complex	453 ± 5	1.4	Crystallization age of foliated granitic sill
04-380	Figure 10	31°34′45.31″S, 67°52′50.36″W	Central Complex	1166 ± 15	–	Crystallization age of foliated orthogneiss
				Lu-Hf Garnet		
PdP13-3	Figure 4	31°20′58.32″S, 68°09′37.72″W	Caucete Group	468 ± 1.9	1.4	Prograde garnet metamorphic age
PdP4-15	Figure 7	31°24′20.34″S, 68°04′06.04″W	Pie de Palo Complex	1067 ± 14	7.2	Metamorphic age from the Duraznos shear zone footwall
PdP4-7	Figure 7	31°24′42.44″S, 68°03′43.47″W	Central Complex	469 ± 21	3.8	Pre-kinematic metamorphic age from the Duraznos shear zone hanging wall
				$^{40}Ar/^{39}Ar$ *Amphibole*		
PdP4-7	Figure 7	31°24′42.44″S, 68°03′43.47″W	Central Complex	441 ± 16	1.4	Inverse isochron age of synkinematic amphibole, p = 0.13
				$^{40}Ar/^{39}Ar$ *Muscovite*		
ASR0216	Figure 4	31°23′30.21″S, 68°06′54.61″W	Caucete Group	417 ± 2	–	Average age, no plateau produced. Equivalent isochron age of 415 ± 2 Ma.
PdP4-7	Figure 7	31°24′42.44″S, 68°03′43.47″W	Central Complex	436 ± 4	0.52	Weighted mean age of four plateau ages, p = 0.60
ASR05a	Figure 8	31°22′57.33″S, 67°48′30.09″W	Central Complex	416 ± 2	–	Plateau age
ASR103c	Figure 10	31°35′15.12″S, 67°5126.27″W	Nikizanga Group	439 ± 7	1.8	Plateau age, p = 0.17
				$^{40}Ar/^{39}Ar$ *Biotite*		
PdP4-7	Figure 7	31°24′42.44″S, 68°03′43.47″W	Central Complex	546 ± 9; 552 ± 9; 526 ± 20	1.2; 0.81; 0.7	Plateau age of synkinematic biotite, p = 0.28; plateau age of synkinematic biotite, p = 0.58; inverse isochron age of synkinematic biotite, p = 0.76
ASR103c	Figure 10	31°35′15.12″S, 67°5126.27″W	Nikizanga Group	255 ± 9; 313 ± 5	1.2; 0.95	Plateau age, p = 0.29; plateau age, p = 0.44

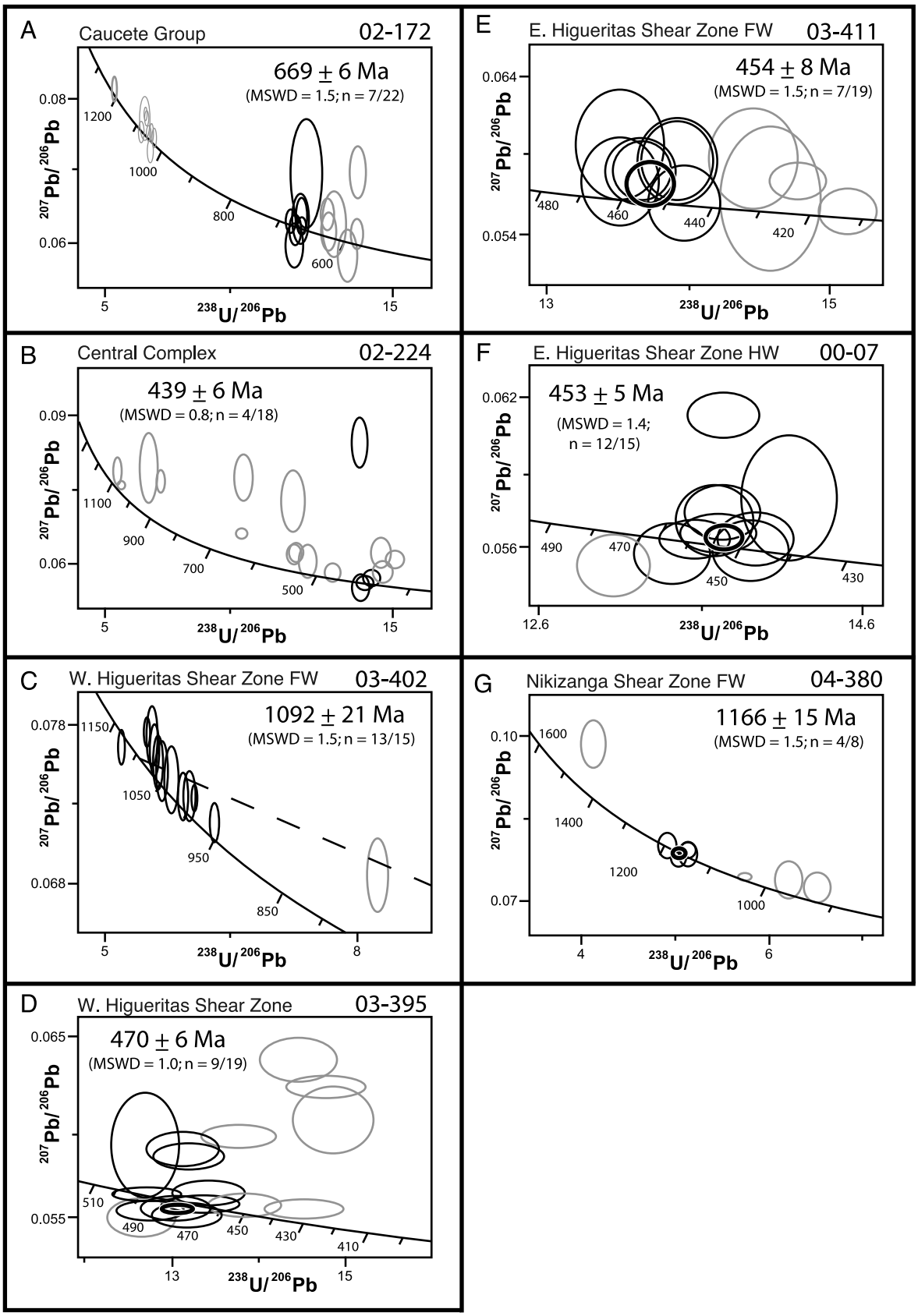
A
Caucete Group
02-172
669 ± 6 Ma
(MSWD = 1.5; n = 7/22)
B
Central Complex
02-224
439 ± 6 Ma
(MSWD = 0.8; n = 4/18)
C
W. Higueritas Shear Zone FW
03-402
1092 ± 21 Ma
(MSWD = 1.5; n = 13/15)
D
W. Higueritas Shear Zone
03-395
470 ± 6 Ma
(MSWD = 1.0; n = 9/19)
E
E. Higueritas Shear Zone FW
03-411
454 ± 8 Ma
(MSWD = 1.5; n = 7/19)
F
E. Higueritas Shear Zone HW
00-07
453 ± 5 Ma
(MSWD = 1.4;
n = 12/15)
G
Nikizanga Shear Zone FW
04-380
1166 ± 15 Ma
(MSWD = 1.5; n = 4/8)
207Pb/206Pb
238U/206Pb

Figure 14

suggest the Duraznos shear zone separates rocks of distinctly different protolith age (~1175 Ma in the footwall compared to ~1060 Ma in the hanging wall).

[37] Syndeformational and postdeformational granitoids within the Sierra de Pie de Palo largely overlap with the magmatic ages from the Famatina arc. The granitoids are generally older along the eastern margin (~454 to ~480 Ma) and younger within the center of the Sierra (439 Ma) (Figure 3). The U-Pb age of 470 ± 6 Ma from a synkinematic granitoid from within the Higueritas shear zone is consistent with a U-Pb zircon age of the El Indio granitoid (481 ± 6 Ma), a biotite granite exposed along strike to the south that intrudes metasedimentary units in the footwall of the Nikizanga shear zone (Figure 10) [*Pankhurst and Rapela*, 1998].

5.2. Lu-Hf Geochronology

[38] We present Lu-Hf isotope data from one sample within the Caucete Group and two samples within the Duraznos shear zone in order to determine the timing of metamorphism and constrain the age of deformation within the units. Four garnet and three garnet-free whole rock separates were analyzed from each sample. Sample Lu-Hf chemistry and analysis of isotopic compositions using the Thermo-Finnigan NEPTUNE were performed at Washington State University where all the procedures are established and routine. Purified garnet and garnet-free whole rock fractions were digested using tabletop dissolution in Savillex beakers to avoid incorporation of Hf from refractory inclusions such as rutile and zircon. Two of the three whole rock fractions from each sample were digested in Teflon bombs to assess the effect of common Hf bound in phases such as zircon and rutile. Removal of the whole rock fractions digested in Teflon bombs from any of the isochrons had no effect on the calculated ages. Lu-Hf isotopic data for the garnet and whole rock separates are given in the auxiliary material and an isochron for each sample is shown in Figure 15. Lu-Hf ages and ϵ_{Hf} values were calculated using a value for the ^{176}Lu decay constant value of 1.867×10^{-11} a^{-1} [*Scherer et al.*, 2001; *Söderlund et al.*, 2004] and $^{176}Hf/^{177}Hf = 0.282785$ and $^{176}Lu/^{177}Hf = 0.0336$ for CHUR (chondrite uniform reservoir) [*Bouvier et al.*, 2008]. The mean square weighted deviation (MSWD) calculated for each regression are greater than a value of 1.0 (Figure 15). Similar values are commonly observed in garnet Lu-Hf isochrons with large ranges in Lu/Hf ratios and low analytical uncertainties. Similarly, theoretical isochron diagrams for Lu-Hf also exhibit high MSWDs [*Kohn*, 2009] and indicate that the geological uncertainties exceed analytical uncertainties in such samples.

[39] Within the Caucete Group, sample PdP13-3, a metavolcanic from the La Paz member, contains a single population of garnet that records prograde metamorphism at conditions of 6.2 ± 1.5 kbar and 524 ± 18°C. The sample yielded an isochron age of 468.0 ± 1.9 Ma (MSWD = 1.4) with an initial $^{176}Hf/^{177}Hf$ of 0.28299 (ϵ_{Hf} = 18) (Figure 15a).

[40] We targeted garnet cores of prekinematic garnet from a metavolcanic member of the Pie de Palo Complex in the footwall of the Duraznos shear zone by picking from grain-size fractions larger than second-generation garnet. Overgrowths on the garnet rims were optically distinct and mechanically broken off the core separates. Sample PdP4-15, from the footwall of the Duraznos shear zone (Figures 7 and 11) yielded an isochron age of 1067 ± 14 Ma (MSWD = 7.2) with an initial $^{176}Hf/^{177}Hf$ of 0.28231 (ϵ_{Hf} = 7.3) (Figure 15b).

[41] Lastly, we sampled prekinematic garnet cores from a metavolcanic member of the Central Complex in the Duraznos hanging wall by picking optically inclusion free garnet. Rims were clearly visible due to abundant intergrowth of matrix muscovite and biotite. Sample PdP4-7, prekinematic garnet from the hanging wall of the Duraznos shear zone (Figures 7 and 11) yielded an isochron age of 469 ± 21 Ma (MSWD = 3.8) with an initial $^{176}Hf/^{177}Hf$ of 0.28233 (ϵ_{Hf} = −5.3) (Figure 15c).

[42] The garnet age of 468.0 ± 1.9 Ma from the Caucete Group records metamorphism of the unit at 6.2 ± 1.5 kbar and 524 ± 18°C. The garnet ages from the Duraznos shear zone are consistent with the break in metamorphic conditions (Figures 13a and 13b) and protolith ages across the shear zone (Figure 13c). The age 469 ± 21 Ma of prekinematic garnet in hanging wall constrains the maximum age of deformation on the Duraznos shear zone.

5.3. The $^{40}Ar/^{39}Ar$ Geochronology

[43] Samples were collected across the transect for $^{40}Ar/^{39}Ar$ geochronology to constrain the cooling history from peak metamorphic temperatures and timing of low-temperature deformation. Samples ASR0216 and ASR05a were analyzed by A. Iriondo while at the U.S. Geological Survey Thermochronology lab in Denver, Colorado. Samples PdP4-7 and ASR103c were analyzed by F. Jourdan while at the Berkeley Geochronology Center at the University of California, Berkeley. Detailed methods are given in the auxiliary material.

[44] Sample ASR0216 is a Ms-Pl-Ep-Qtz schist from the southern Caucete Group window (Figure 4). Muscovite forms a well-defined stretching lineation, defines the foliation with alternating quartz-rich horizons (Figure 9d), and occurs as tails on plagioclase and epidote porphyroclasts. The muscovite separate did not result in a plateau but produced an average age of 417 ± 2 Ma, representing ~82.6% of the total gas released (Figure 16a). The inverse isochron produced equivalent results (415 ± 2 Ma, MSWD = 37; Figure 16b).

Figure 14. Zircon U-Pb diagrams for igneous and metaigneous samples from the Sierra de Pie de Palo. (a) Metadacite/rhyolite of the Caucete Group exposed in the easternmost Caucete Group window in Quebrada Molle (Figure 4). (b) Pegmatitic leucogranite dike that cross cuts a fold in the Central Complex (Figures 2 and 5h). (c) Metavolcanic/volcaniclastic from the Central Complex in Quebrada Higueritas (Figure 8). (d) Granitic sills whose geometry defines an S-C fabric within the western Higueritas shear zone (Figures 5g and 8). (e) Weakly foliated granodiorite sill from within Quebrada Higueritas (Figure 8). (f) Foliated granitic sill of the Central Complex exposed on the eastern margin of the Sierra de Pie de Palo (Figure 8). (g) Foliated orthogneiss in the footwall of the Nikizanga shear zone (Figure 10).

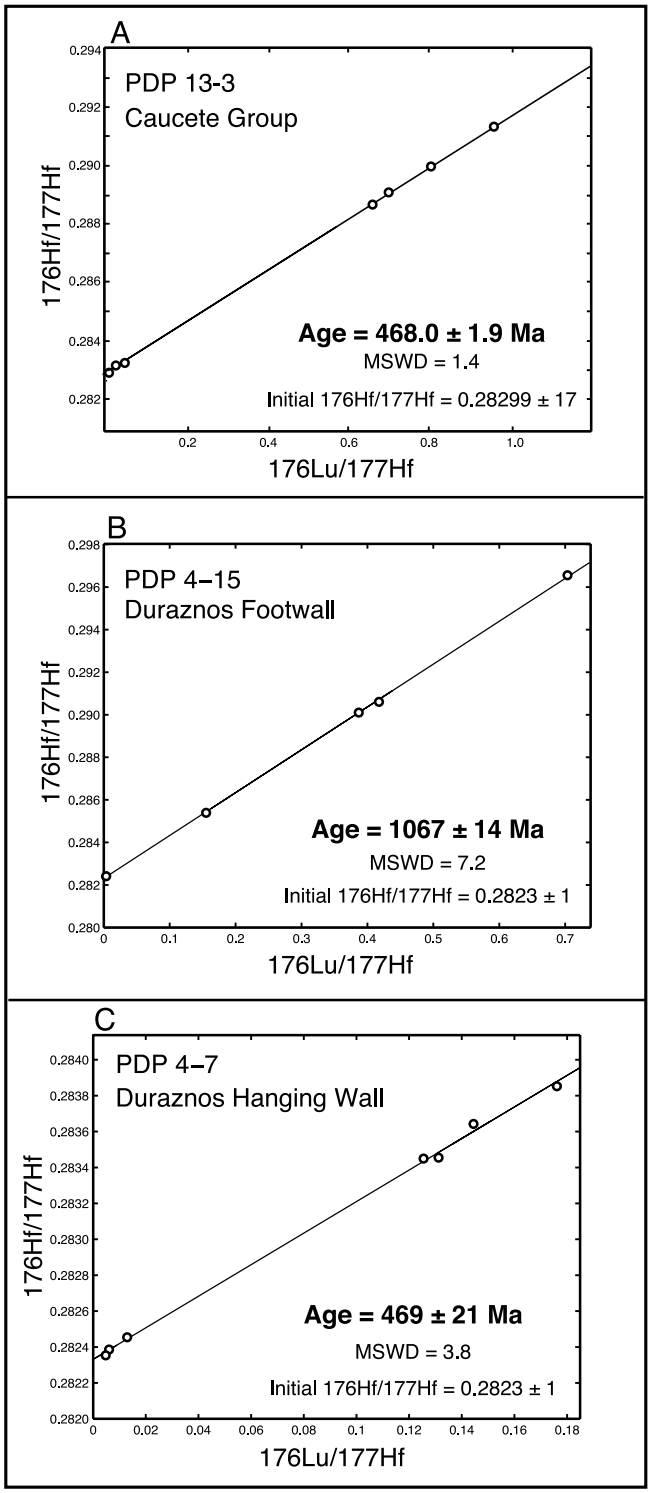

Figure 15. Lu-Hf isochrons for (a) sample PdP13-3 from the Caucete Group (Figure 3), (b) sample PdP4-15 from the footwall of the Duraznos shear zone (Figure 8), and (c) sample PdP4-7 from the hanging wall of the Duraznos shear (Figure 8).

[45] Sample PdP4-7 is from a metavolcanic member of the Central Complex in the hanging wall of the Duraznos shear zone and is described above. Amphibole, muscovite, and biotite define a mineral lineation in hand sample and outcrop. The three minerals are intergrown with the mylonitic mineral assemblage and occur as asymmetric tails on prekinematic porphyroclasts. The amphibole separate shows evidence for excess argon and failed to produce well-defined plateau and (Figure 15a). The inverse isochron technique accounts for excess argon in the calculation [*Heizler and Harrison*, 1988] and resulted in an age of 441 ± 16 Ma (MSWD = 1.4; p = 0.13) and an $^{40}Ar/^{36}Ar$ intercept of 3500 ± 300 (Figure 16b). Four muscovite separates produced plateau ages ranging from 434 ± 8 Ma to 439 ± 7 Ma (Figure 16a) from which we calculated a weighted mean age of 436 ± 4 Ma (MSWD = 0.52, p = 0.60). Isochrons for the muscovite separates failed to provide reliable ages as the data cluster exclusively near the radiogenic axis (Figure 16b). Two of three biotite separates produced ages of 546 ± 9 Ma (MSWD = 1.2, p = 0.28) and 552 ± 9 Ma (MSWD = 0.81,p = 0.58). The third separate failed to produce a plateau and gave an average age of ~558 Ma. An inverse isochron for the third separate produced an age of 526 ± 20 (MSWD = 0.66; p = 0.76) and a $^{40}Ar/^{36}Ar$ intercept of 1000 ± 400.

[46] Sample ASR05a is from the same location as U-Pb sample 00-07 within the East Higueritas shear zone (Figure 8). The orthogneiss is a recrystallized Bt-Ms-Pl-Ep-Qtz schist of the Central Complex. Muscovite wraps plagioclase porphyroclasts and defines a mineral stretching lineation in outcrop (Figure 9e). Quartz preserves irregular grain shapes and lobate boundaries indicative of dynamic recrystallization by grain boundary migration and indicates relatively high temperatures of deformation (>400°C). Two muscovite separates were analyzed; one did not form a plateau and gave an average age of 417 ± 2 Ma, the other resulted in plateau with an age of 416 ± 2 Ma (Figure 16a). Inverse isochrons for the separates produced equivalent results of 415 ± 2 Ma (MSWD 2.4) and 415 ± 2 Ma (MSWD = 2.0) (Figure 16b).

[47] Sample ASR103c is a Ms-Bt-Chl-Qtz schist of the Nikizanga Group from the hanging wall of the Nikizanga shear zone (Figure 10). Muscovite and biotite define a mineral stretching lineation, are aligned in the foliation, and muscovite forms asymmetric mica fish (Figure 9f). Muscovite produced a plateau age of 439 ± 7 Ma (MSWD = 1.8, p = 0.17) representing ~67% of the total gas released (Figure 15a) and an equivalent inverse isochron age of 439 ± 6 Ma (MSWD = 0.98, p = 0.47) with an initial $^{40}Ar/^{36}Ar$ ratio of 290 ± 30 (Figure 15b). Two biotite separates from the sample gave plateau ages of 255 ± 9 Ma (MSWD = 1.21, p = 0.29) and 313 ± 5 Ma (MSWD = 0.95, p = 0.44) (Figure 16a) with 69% and 52% of the total gas released, respectively.

6. Discussion

6.1. Deformation Within the Sierra de Pie de Palo

[48] In what follows, we combine the above magmatic ages with Lu-Hf geochronology and $^{40}Ar/^{39}Ar$ thermochronology to constrain the absolute timing of deformation along the

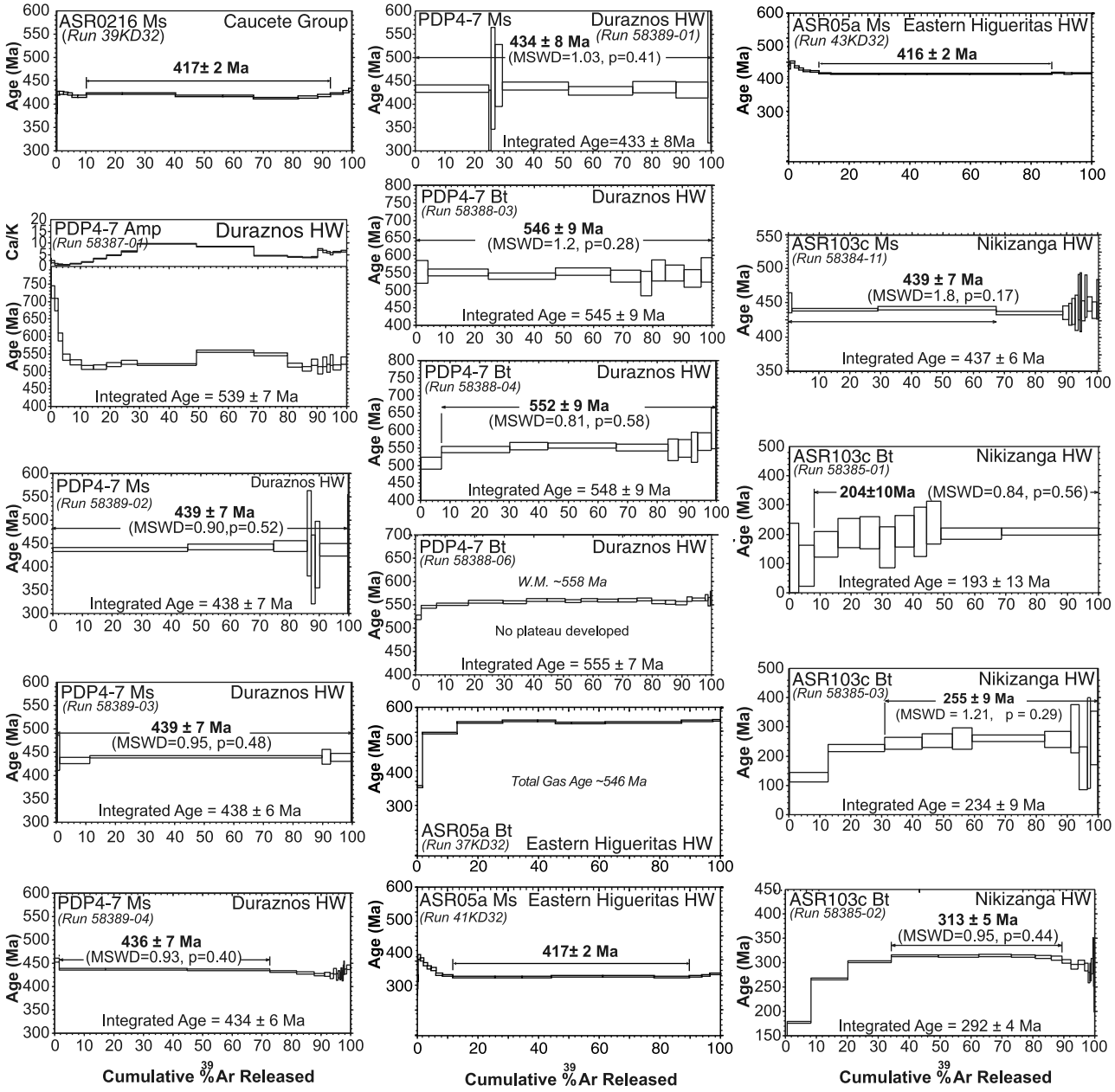

Figure 16. (a) The $^{40}Ar/^{39}Ar$ age spectra and (b) inverse isochrons for muscovite, biotite, and amphibole separates throughout the study area.

individual shear zones. We discuss the timing of deformation from west to east and a summary is shown in Figure 17.

[49] Deformation on the retrograde shear zone of the Las Pirquitas thrust that juxtaposes the Caucete Group in the footwall against older mylonites and ultramylonites in the Pie de Palo Complex is likely one of the youngest structures examined in this study (Figure 17). The shear zone truncates older mylonitic fabrics in both the hanging wall and footwall at the range front as well as fabrics associated with the Pie de Palo thrust at the location of the windows. *Mulcahy et al.* [2007] documented a Cambrian (~515 Ma) mylonite event preserved within the hanging wall of the Las Pirquitas thrust (Figures 3 and 4), now multiply folded and subsequently deformed by the younger retrograde shear zone. Cambrian deformation occurred at 9 kbar and ~500°C [*Mulcahy et al.*, 2007], consistent with the P-T conditions of the Pie de Palo complex found in this study. The muscovite $^{40}Ar/^{39}Ar$ of 417 ± 2 Ma from the structural window of the Caucete Group gives a minimum age of deformation because the fine-grained, uniform composition muscovite formed at temperature above its nominal closure temperature (~350 ± 50° depending on cooling rate [*McDougall and Harrison*, 1999]).

[50] Deformation on the Pie de Palo thrust is constrained to be synchronous or slightly older than top-to-the-east exten-

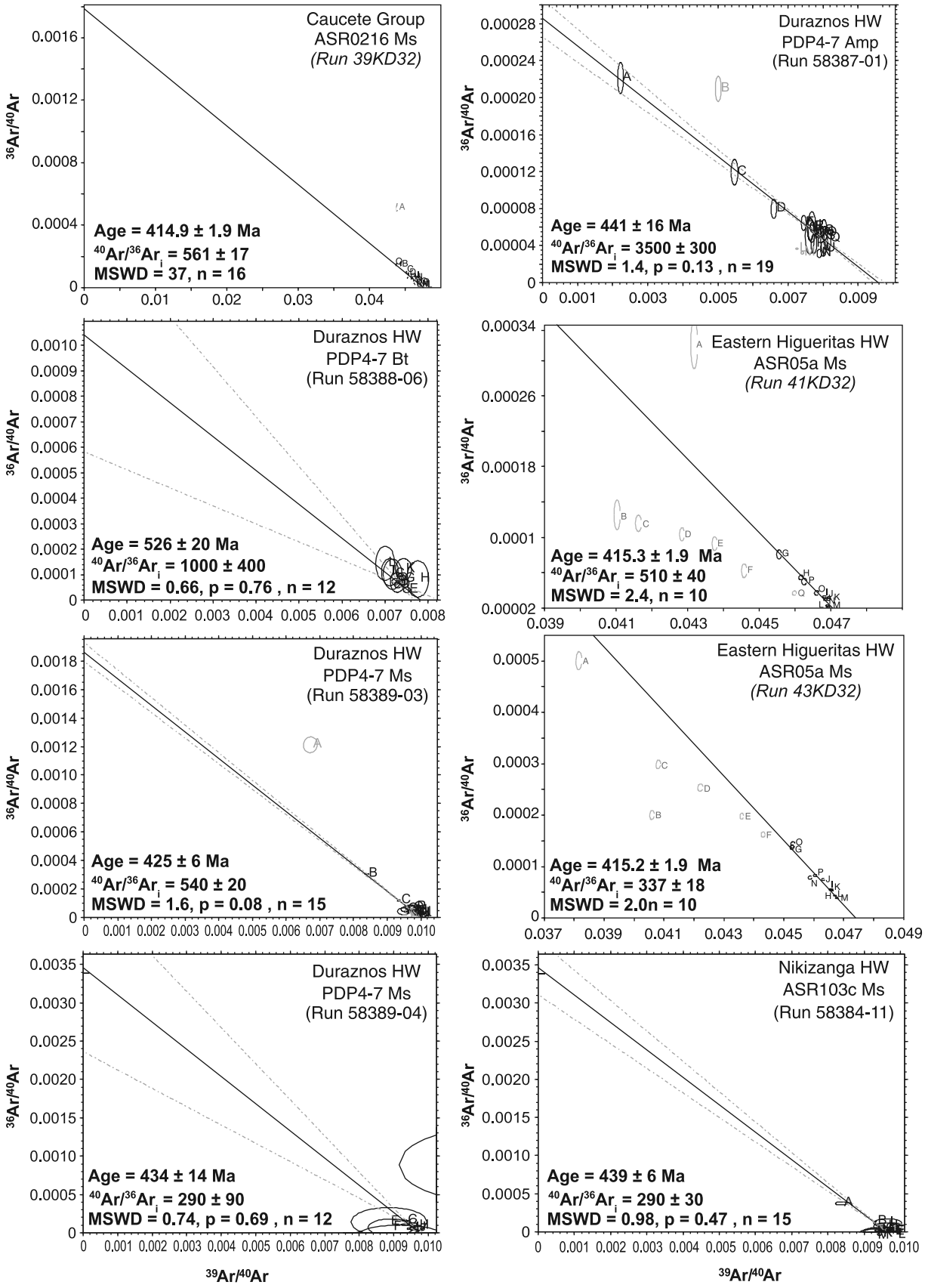

Figure 16. (continued)

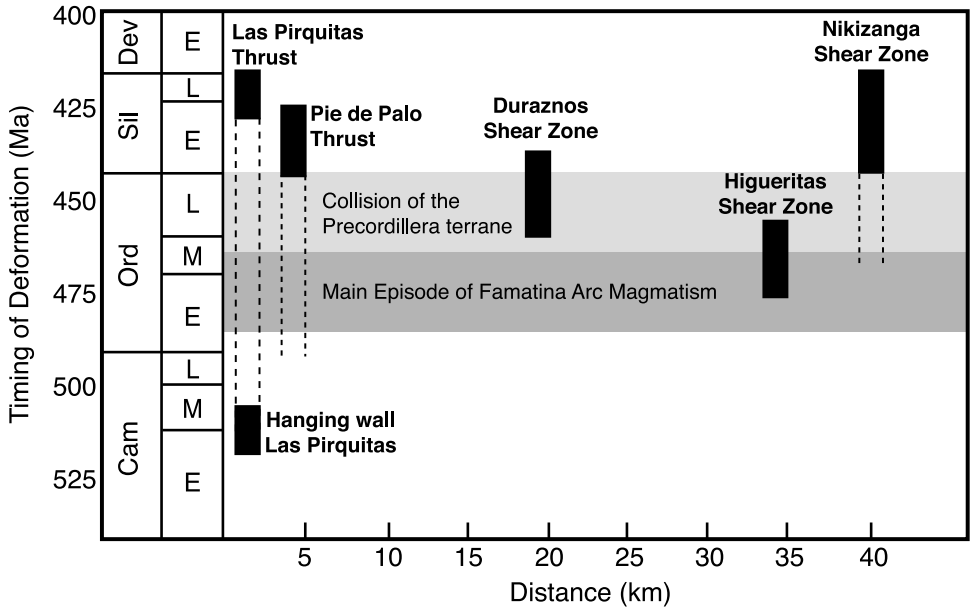

Figure 17. Timing of deformation on individual structures within the Sierra de Pie de Palo as constrained by the geochronology depicted in Figure 3.

sion on the Nikizanga shear zone and to predate deformation on the retrograde shear zone of the Las Pirquitas thrust (Figure 17). Within the footwall of the Pie de Palo thrust, sample PdP12-5 (Figure 3) is strongly overprinted by the mylonitic fabric associated with the shear zone. Pressure-temperature conditions of ~560°C and ~8.4 kbar for this sample indicate that deformation on the Pie de Palo thrust may have began prior to extension and exhumation on the Nikizanga shear zone (Figure 17).

[51] Deformation on the Duraznos shear zone is bracketed to be younger than 469 ± 21 Ma and greater than ~441–439 Ma (Figure 17). The hanging wall of the Duraznos shear zone records prekinematic garnet growth at 469 ± 21 Ma, evidenced by straight internal foliation within garnet at a high angle to the mylonitic shear zone foliation associated with shear zone. The garnet age overlaps with top-to-the-west thrusting on the Higueritas shear zone and we interpret the garnet growth as a result of burial during that event. Amphibole and white mica $^{40}Ar/^{39}Ar$ ages of 441 ± 6 Ma and 436 ± 4 Ma, respectively, are likely cooling rather than crystallization ages as deformation along the Duraznos shear zone occurred at temperatures above the accepted closure temperatures for both minerals. Biotite from the same sample produced $^{40}Ar/^{39}Ar$ ages of 546 ± 9 Ma and 552 ± 9 Ma that are older than the prekinematic garnet Lu-Hf age. These older ages are interpreted to be the result of a low-temperature deformation or fluid event that resulted in the incorporation of excess argon in biotite. Isoclinal recumbent folding within the hanging wall of Duraznos shear zone ended by ~439 Ma as evidenced by U-Pb zircon ages from an undeformed pegmatitic granitoid that cross cuts a fold hinge in the hanging wall (Figure 5h). The combined Lu-Hf garnet geochronology and $^{40}Ar/^{39}Ar$ thermochronology from sample PdP4-7, within the immediate hanging wall of the Duraznos shear zone, indicate a rapid phase of Late Ordovician cooling consistent with *Casquet et al.* [2001], who inferred that top-to-the-west deformation within the Central Complex occurred during conditions of decreasing pressure.

[52] Initiation of the western Higueritas shear zone is constrained to be older than or equal to ~470 Ma although deformation may have occurred until 454 ± 8 Ma (Figure 17). Zircon U-Pb ages from synkinematic granitoids within the westernmost mylonite zone (Figures 8 and 5g) date the initiation of top-to-the-west thrusting by 470 ± 6 Ma. Deformation occurred at high pressures (~13 kbar) and temperatures (~734°C) in the presence of melt. The replacement of kyanite by sillimanite is consistent with isothermal decompression and/or with heating during emplacement of granitic melts during deformation.

[53] The weakly foliated granitoid with a U-Pb zircon age of ~454 Ma may either mark late stage deformation on the western Higueritas shear zone or overprinting from younger deformation associated with the eastern Higueritas shear zone. The eastern margin of the eastern Higueritas shear zone includes penetratively deformed and recrystallized orthogneiss with a U-Pb age of ~454 Ma. The timing of top-to-the-west thrusting on the eastern Higueritas shear is thus poorly constrained but is likely coeval with or postdates the western shear zone. Top-to-the-east kinematic indicators in the eastern Higueritas shear zone may be related to a younger extensional deformation associated with the Nikizanga shear zone (see below). This, however, remains to be tested with a more detailed study.

[54] Top-to-the-east extension on the Nikizanga shear zone is constrained to have occurred between 436 ± 4 Ma and 415 ± 2 Ma (Figure 17). Rapid cooling in the Duraznos hanging wall was synchronous with the $^{40}Ar/^{39}Ar$ white mica cooling age from the Nikizanga shear zone. In addition,

mylonitic pressures of ~9 kbar within the Duraznos shear zone are lower than premylonitic conditions of ~13 kbar reported by *Casquet et al.* [2001]. The observations suggest that considerable exhumation along the Nikizanga shear zone occurred prior to deformation within the Duraznos shear zone or unrecognized structures exist between the Duraznos shear zone and the Nikizanga and Higueritas shear zones. Although P-T data are lacking from the hanging wall of the Nikizanga shear zone, the presence of melt in the footwall (e.g., the El Indio granitoid), and pressure solution fabrics in the hanging wall indicate a substantial break in temperature across the shear zone. Continued exhumation and cooling are interpreted to have occurred to at least ~417–415 Ma, as indicated by white mica cooling ages along both the eastern margin and within the Caucete Group exposed within windows of the Las Pirquitas thrust along the western portion of the range (Figure 3).

6.2. Evolution of the Famatina Margin

[55] The deformation history preserved within the Sierra de Pie de Palo can be correlated to the magmatic and deformation history of the Famatina margin and to the accretion history of the Precordillera terrane (Figure 18). Cambrian mylonites within the Pie de Palo Complex coincide with initiation of the Famatina arc and establishment of a convergent margin [*Mulcahy et al.*, 2007]. The mylonites crystallized under relatively high P/T conditions that we interpret as forming during initial establishment of the convergent margin. On this basis, and the absence of middle Cambrian deformation within the Precordillera terrane, *Mulcahy et al.* [2007] suggested that the Pie de Palo block was part of the Famatina margin by ~515 Ma (Figure 18a) and was not part of the Precordillera terrane.

[56] Oblique, top-to-the-west thrusting within the western Higueritas shear zone initiated at or prior ~470 Ma and was either continuous or protracted until ~454 Ma. This period is synchronous with voluminous magmatism within the Famatina arc (~485–465 Ma) [*Ducea et al.*, 2010], east vergent retro-arc thrusting (~470 Ma) [*Astini and Dávila*, 2004], and initial collision of the Precordillera terrane (~470 Ma) [*Fanning et al.*, 2004] (Figure 18b).

[57] Following deformation on the western Higueritas shear zone, deformation stepped westward to the Duraznos shear zone between 469 ± 21 Ma and 441 ± 16 Ma (Figure 18c). Oblique, top-to-the-west thrusting on the Duraznos shear zone overlaps with the end of voluminous arc magmatism (~465 Ma) [*Ducea et al.*, 2010] and with west directed thrusting in Late Ordovician (~458–449 Ma) sediments of the Precordillera terrane [*Thomas and Astini*, 2007]. The data support that the Precordillera had fully collided with the Famatina arc margin by that time and may have led to the cessation of voluminous magmatism within the Famatina arc.

[58] Top-to-the east extension along the Nikizanga shear zone, synchronous with down-dip convergence along lower-grade shear zones at ~436 Ma, broadly coincides with the cessation of accretion of the Precordillera terrane [*Astini*, 1998] and the end of magmatism within the Famatina arc [*McClelland et al.*, 2005]. This time period may mark the establishment of a new plate margin west of the Precordillera terrane and the closing of an ocean basin between the Precordillera and the outboard Chilenea terrane [e.g., *Davis et al.*, 1999].

6.3. Affinity of the Sierra de Pie de Palo

[59] On the basis of stratigraphic correlations and detrital zircon ages, the Caucete Group is considered to represent the metamorphosed equivalent of Paleozoic rocks within the Precordillera terrane to the west [e.g., *Ramos et al.*, 1998; *Vujovich and Kay*, 1998; *Naipauer et al.*, 2010; *van Staal et al.*, 2010]. The affinity of the Pie de Palo Complex, Central Complex, and Nikizanga Group, however, are considered as either (1) original basement to the Precordillera terrane or (2) separate from the Precordillera terrane and to have been part of the Famatina margin by ~515 Ma.

[60] The Precordillera terrane is commonly accepted to have rifted from Laurentia in the Late Cambrian and to have remained as an isolated thermally subsiding passive margin until ~470 Ma [*Astini and Thomas*, 1999; *Benedetto et al.*, 1999] where the presence of Middle Ordovician K-bentonites [*Huff et al.*, 1998; *Fanning et al.*, 2004] and drowning of the carbonate platform [*Astini and Thomas*, 1999] are interpreted to mark its approach and initial accretion, respectively, to the Famatina margin. *Mulcahy et al.* [2007] argued on the basis of a Cambrian (~515 Ma) mylonite event in the hanging wall of the Las Pirquitas thrust that the Pie de Palo block could not be part the Precordillera, which lacks evidence of middle Cambrian deformation. The relatively high P/T conditions of the Cambrian mylonite event are consistent with having formed in a convergent margin setting. Based on similar ages of metamorphism and magmatism throughout the Famatina margin, the authors hypothesized the Pie de Palo is more consistent with being adjacent to the Famatina margin by that time.

[61] Data from this study support the latter argument. Distinct breaks in protolith and metamorphic ages occur across major structures implying that the Sierra de Pie de Palo is composed of distinct tectonic slices rather than comprising an intact ophiolite and cover sequence. Zircon U-Pb ages from syndeformational and postdeformational granitoids throughout the Sierra de Pie de Palo generally young toward the foreland and overlap with the magmatic ages from the Famatina arc. The P-T conditions of deformation within the western Higueritas shear zone places those rocks at lower crustal conditions and relatively high temperatures prior to or synchronous with initial drowning of the Precordillera platform. Taken together, the long-lived tectonic history within the Pie de Palo block, exclusive of the Caucete Group, records the evolution of a fore arc from subduction to arc-continental collision.

7. Conclusions

[62] The Sierra de Pie de Palo preserves a middle to lower crustal imbricate section composed of distinct lithotectonic units that were juxtaposed throughout a prolonged history of deformation. Deformation occurred intermittently from ~515 to 417 Ma. The deformation, metamorphic, and magmatic record are consistent with regional models that place rocks of the Sierra de Pie de Palo (excluding the Caucete Group) ad-

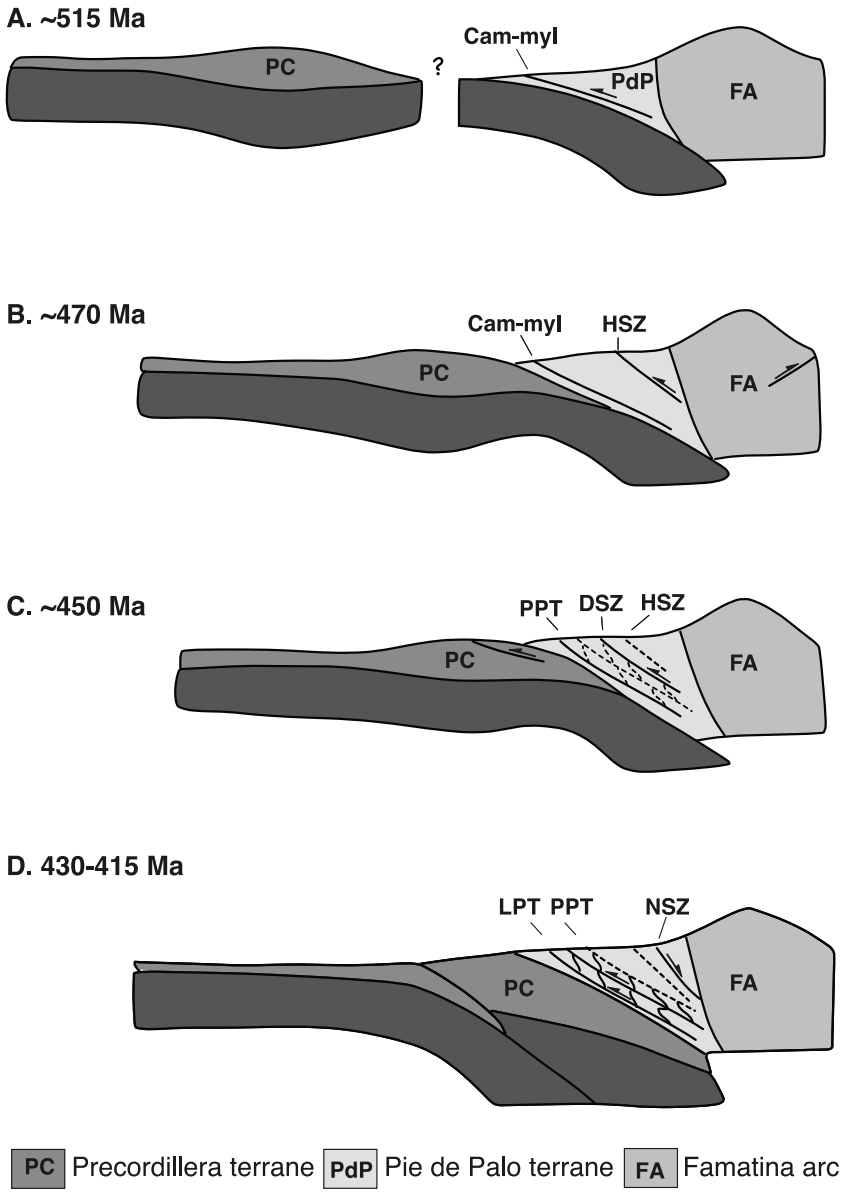

Figure 18. (a–d) Tectonic model for the structural evolution of the Pie de Palo block and timing of individual structures with respect to the accretion of the Precordillera terrane and evolution of the Famatina margin. Abbreviations are as follows: PC, Precordillera; PdP, Pie de Palo block; FA, Famatina arc; Cam-myl, Cambrian mylonites within the hanging wall of the Las Pirquitas thrust; HSZ, Higueritas shear zone; DSZ, Duraznos shear zone; PPT, Pie de Palo thrust; LPT, Las Pirquitas thrust; NSZ, Nikizanga shear zone. See text for discussion.

jacent to the Famatina margin and not basement to the Precordillera terrane. Additionally, Paleozoic intrusive ages within the Sierra de Pie de Palo overlap with magmatic ages from the Famatina arc, which are more consistent with it occupying an upper plate position during accretion of the Precordillera terrane. Juxtaposition of the Caucete Group and rocks of the Pie de Palo and Central complex along the retrograde Las Pirquitas thrust is constrained to have occurred between ~436 Ma and ~417 Ma.

[63] The deformation history preserved within the Sierra de Pie de Palo supports existing models of Cordilleran margins that invoke arc flare-up linked to episodes of regional shortening. Early top-to-the-west deformation along oblique thrusts in the Sierra de Pie de Palo (~470–450 Ma) was broadly synchronous with voluminous arc magmatism and retro-arc shortening. This episode of increased magmatism ceased with the onset accretion of the Precordillera terrane and synconvergent extension within the Sierra de Pie de Palo. Continued synextensional to postextensional convergence was accommodated along progressively lower grade shear zones following terrane accretion and the establishment on a new plate margin west of the Precordillera terrane.

[64] **Acknowledgments.** S. R. Mulcahy is grateful to J. Ellis, Y. Gato, and J. Mescua for their assistance in the field. This research was supported by National Science Foundation grants 0126198 to S. M. Roeske and 0126299 to W. C. McClelland. A. Iriondo would like to thank Mick Kunk from the U.S. Geological Survey Thermochronology Lab for his help obtaining and interpreting the Ar-Ar data for this study. We thank E. S. Cowgill and H. W. Day for comments on early versions of the manuscript. We thank V. Ramos and M. Williams for their critical and insightful reviews and R. Miller and T. Ehlers for their comments and editorial management.

References

Astini, R. A. (1998), Stratigraphical evidence supporting the rifting, drifting and collision of the Laurentian Precordillera terrane of western Argentina, *Geol. Soc. Spec. Publ.*, *142*, 11–33.

Astini, R. A., and F. M. Dávila (2004), Ordovician back arc foreland and Ocloyic thrust belt development on the western Gondwana margin as a response to Precordillera terrane accretion, *Tectonics*, *23*, TC4008, doi:10.1029/2003TC001620.

Astini, R. A., and W. A. Thomas (1999), Origin and evolution of the Precordillera terrane of western Argentina: A drifted Laurentian orphan, in *Laurentia-Gondwana Connections Before Pangea*, edited by V. A. Ramos and J. D. Keppie, *Spec. Pap. Geol. Soc. Am.*, *336*, 1–20.

Astini, R. A., J. L. Benedetto, and N. E. Vaccari (1995), The Early Paleozoic evolution of the Argentine Precordillera as a Laurentian rifted, drifted, and collided terrane: A geodynamic model, *Geol. Soc. Am. Bull.*, *107*, 253–273.

Benedetto, J. L., T. M. Sanchez, M. G. Carrera, E. D. Brussa, and M. J. Salas (1999), Paleontological constraints on successive paleogeographic positions of Precordillera terrane during the early Paleozoic, in *Laurentia-Gondwana Connections Before Pangea*, edited by V. A. Ramos and J. D. Keppie, *Spec. Pap. Geol. Soc. Am.*, *336*, 21–42.

Bouvier, A., J. D. Vervoort, and P. J. Patchett (2008), The Lu-Hf and Sm-Nd isotopic composition CHUR: Constraints from unequilibrated chondrites and implications for the bulk composition of terrestrial planets, *Earth Planet. Sci. Lett.*, *273*, 48–57.

Casquet, C., E. Baldo, R. J. Pankhurst, C. W. Rapela, C. Galindo, C. M. Fanning, and J. Saavedra (2001), Involvement of the Argentine Precordillera terrane in the Famatinian mobile belt: U-Pb SHRIMP and metamorphic evidence from the Sierra de Pie de Palo, *Geology*, *29*, 703–706.

Dalla Salda, L., and R. Varela (1984), El metamorfismo en el tercio sur de la sierra de Pie de Palo, San Juan, *Asoc. Geol. Argent. Rev.*, *39*, 68–93.

Davis, J. S., S. M. Roeske, W. C. McClelland, and L. W. Snee (1999), Closing the ocean between the Precordillera terrane and Chilenia: Early Devonian ophiolite emplacement and deformation in the southwest Precordillera, in *Laurentia-Gondwana Connections Before Pangea*, edited by V. A. Ramos and J. D. Keppie, *Spec. Pap. Geol. Soc. Am.*, *336*, 115–138.

DeCelles, P. G., M. N. Ducea, P. Kapp, and G. Zandt (2009), Cyclicity in Cordilleran orogenic systems, *Nat. Geosci.*, *2*, 251–257.

Ducea, M. N. (2001), The California arc: Thick granitic batholiths, eclogitic residues, lithospheric-scale thrusting, and magmatic flare-ups, *GSA Today*, *11*, 4–10.

Ducea, M. N., and M. D. Barton (2007), Igniting flare-up events in California arcs, *Geology*, *35*, 1047–1050.

Ducea, M. N., J. E. Otamendi, G. Bergantz, K. M. Stair, V. A. Valencia, and G. E. Gehrels (2010), Timing constraints on building an intermediate plutonic arc crustal section: U-Pb zircon geochronology of the Sierra Valle Fértil–La Huerta, Famatinian Arc, Argentina, *Tectonics*, *29*, TC4002, doi:10.1029/2009TC002615.

Fanning, C. M., R. J. Pankhurst, C. W. Rapela, E. G. Baldo, C. Casquet, and C. Galindo (2004), K-bentonites in the Argentine Precordillera contemporaneous with rhyolite volcanism in the Famatinian Arc, *J. Geol. Soc.*, *161*, 747–756.

Galindo, C., C. Casquet, C. W. Rapela, R. J. Pankhurst, E. Baldo, and J. Saavedra (2004), Sr, C, and O isotope geochemistry and stratigraphy of Precambrian and lower Paleozoic carbonate sequences from the western Sierras Pampeanas of Argentina: Tectonic implications, *Precambrian Res.*, *131*, 55–71.

Huff, W. D., S. M. Bergstrom, D. R. Kolata, C. A. Cingolani, and R. A. Astini (1998), Ordovician K-bentonites in the Argentine Precordillera: Relations to Gondwana margin evolution, in *The Proto-Andean margin of Gondwana*, edited by R. J. Pankhurst and C. W. Rapela, *Geol. Soc. Spec. Publ.*, *142*, 107–126.

Kohn, M. J. (2009), Models of garnet differential geochronology, *Geochim. Cosmochim. Acta*, *73*, 170–182.

Kretz, R. (1983), Symbols for rock-forming minerals, *Am. Mineral.*, *68*, 277–279.

McClelland, W. C., S. M. Roeske, G. I. Vujovich, S. R. Mulcahy, and J. R. Ellis (2005), U-Pb SHRIMP evidence for allochthonous elements between the Precordillera terrane and Gondwana margin, Sierra de la Huerta, northwest Argentina, paper presented at GAC-MAC Annual Meeting, Geol. Assoc. of Can., Halifax, N. S., Canada.

McDonough, M. R., V. A. Ramos, C. E. Isachsen, S. A. Bowring, and G. I. Vujovich (1993), Edades preliminares de circones del basamento de la Sierra de Pie de Palo, Sierras Pampeanas occidentales de San Juan: Sus implicancias para el supercontinente Proterozoico de Rodinia, in *XIII Congreso Geológico Argentino y II Congreso de Exploración de Hidrocarburos*, vol. 3, pp. 340–342, Argentine Geol. Congr., Buenos Aires.

McDougall, I., and T. M. Harrison (1999), *Geochronology and Thermochronology by the $^{40}Ar/^{39}Ar$ Method*, Oxford Univ. Press, New York.

Mulcahy, S. R., S. M. Roeske, W. C. McClelland, S. Nomade, and P. R. Renne (2007), Cambrian initiation of the Las Pirquitas thrust of the western Sierras Pampeanas, Argentina: Implications for the tectonic evolution of the proto-Andean margin of South America, *Geology*, *35*, 443–446.

Naipauer, M., G. I. Vujovich, C. A. Cingolani, and W. C. McClelland (2010), Detrital zircon analysis from the Neoproterozoic-Cambrian sedimentary cover (Cuyania terrane), Sierra de Pie de Palo, Argentina: Evidence of a rift and passive margin system?, *J. South Am. Earth Sci.*, *29*, 306–326.

Pankhurst, R. J., and C. W. Rapela (1998), The proto-Andean margin of Gondwana: An introduction, *Geol. Soc. Spec. Publ.*, *142*, 1–9.

Pankhurst, R. J., C. W. Rapela, and C. M. Fanning (2000), Age and origin of coeval TTG, I- and S-type granites in the Famatinian belt of NW Argentina, *Trans. R. Soc. Edinburgh Earth Sci.*, *91*, 151–168.

Powell, R., and T. Holland (1994), Optimal geothermometry and geobarometry, *Am. Mineral.*, *79*, 120–133.

Quenardelle, S. M., and V. A. Ramos (1999), Ordovician western Sierras Pampeanas magmatic belt: Record of Precordillera accretion in Argentina, in *Laurentia-Gondwana Connections Before Pangea*, edited by V. A. Ramos and J. D. Keppie, *Spec. Pap. Geol. Soc. Am.*, *336*, 63–86.

Ramos, V. A. (2004), Cuyania, an exotic block to Gondwana: Review of a historical success and the present problems, *Gondwana Res.*, *7*, 1009–1026.

Ramos, V. A., G. I. Vujovich, and R. D. Dallmeyer (1996), Los klippes y ventanas tectónicas preándicas de la Sierra de Pie de Palo (San Juan): Edad e implicaciones tectónicas, in *XIII Congreso Geológico Argentino y III Congreso de Exploración de Hidrocarburos*, vol. 5, pp. 377–391, Argentine Geol. Congr., Buenos Aires.

Ramos, V. A., R. D. Dallmeyer, and G. Vujovich (1998), Time constraints on the Early Paleozoic docking of the Precordillera, central Argentina, *Geol. Soc. Spec. Publ.*, *142*, 143–158.

Rapela, C. W., R. J. Pankhusrt, C. Casquet, E. Baldo, C. Galindo, C. M. Fanning, and J. M. Dahlquist (2010), The western Sierras Pampeanas: Protracted Grenville-age history (1330–1030 Ma) of intra-oceanic arcs, subduction-accretion at continental-edge and AMCG intraplate magmatism, *J. South Am. Earth Sci.*, *29*, 105–127.

Scherer, E., C. Münker, and K. Mezger (2001), Calibration of the lutetium-hafnium clock, *Science*, *293*, 683–687.

Söderlund, U., P. J. Patchett, J. D. Vervoort, and C. E. Isachsen (2004), The ^{176} Lu decay constant determined by Lu-Hf and U-Pb isotope systematics of Precambrian mafic intrusions, *Earth Planet. Sci. Lett.*, *219*, 311–324.

Thomas, W. A., and R. A. Astini (2007), Vestiges of an Ordovician west-vergent thin-skinned Ocloyic thrust belt in the Argentine Precordillera, southern Central Andes, *J. Struct. Geol.*, *29*, 1369–1385.

van Staal, C. R., G. I. Vujovich, and M. Naipauer (2010), An Alpine-style Ordovician collision complex in the Sierra de Pie de Palo, Argentina: Record of subduction of Cuyania beneath the Famatina arc, *J. Struct. Geol.*, doi:10.1016/j.jsg.2010.10.011, in press.

Varela, R., and L. Dalla Salda (1992), Geocronología Rb-Sr de metamorfitas y granitoides del extremo sur de la Sierra Pie de Palo, San Juan, *Asoc. Geol. Argent. Rev.*, *47*, 271–275.

Vujovich, G. I., and S. M. Kay (1998), A Laurentian? Grenville-age oceanic arc/back-arc terrane in the Sierra de Pie de Palo, western Sierras Pampeanas, Argentina, in *The Proto-Andean Margin of Gondwana*, edited by R. J. Pankhurst and C. W. Rapela, *Geol. Soc. Spec. Publ.*, *142*, 159–180.

Vujovich, G. I., C. R. van Staal, and W. Davis (2004), Age constraints on the tectonic evolution and provenance of the Pie de Palo complex, Cuyania Composite terrane, and the Famatinian orogeny in the Sierra Pie de Palo, San Juan, Argentina, *Gondwana Res.*, *7*, 1041–1056.

A. Iriondo, Centro de Geociencias, Universidad Nacional Autónoma de México, Campus Juriquilla, Querétaro, 76230, Mexico.

F. Jourdan, Western Australian Argon Isotope Facility, Department of Applied Geology and JdL-CMS, Curtin University of Technology, Perth, WA 6845 Australia.

W. C. McClelland, Department of Geoscience, University of Iowa, Iowa City, IA 52242, USA.

S. R. Mulcahy, Department of Earth and Planetary Sciences, University of California, Berkeley, CA 94720-4767, USA. (mulcahy@berkeley.edu)

P. R. Renne, Berkeley Geochronology Center, Berkeley, CA 94709, USA.

S. M. Roeske, Department of Geology, University of California, Davis, CA 95616, USA.

J. D. Vervoort, School of Earth and Environmental Sciences, Washington State University, Pullman, WA 99164, USA.

G. I. Vujovich, Department of Geology, University of Buenos Aires-CONICET, Ciudad Universitaria, C1428EHA Buenos Aires, Argentina.